10-30-2015 12:00 AM

Non-Canonical Activation of Nrf2 by Dimercaptopropanol as a Treatment for Huntington's Disease

Margaret Lauren Tindale, *The University of Western Ontario*

Supervisor: Dr. Robert Cumming, *The University of Western Ontario*

A thesis submitted in partial fulfillment of the requirements for the Master of Science degree in Neuroscience

NON-CANONICAL ACTIVATION OF NRF2 BY DIMERCAPTOPROPANOL AS A TREATMENT FOR HUNTINGTON'S DISEASE

(Thesis format: Monograph)

by

Margaret Lauren Tindale

Graduate Program in Neuroscience

A thesis submitted in partial fulfillment
of the requirements for the degree of
Master of Science

The School of Graduate and Postdoctoral Studies
The University of Western Ontario
London, Ontario, Canada

Abstract

Mitochondrial dysfunction and elevated reactive oxygen species (ROS) levels are strongly implicated in various neurodegenerative disorders, including Huntington's disease (HD). Expression of the mutant Huntingtin protein (mHTT) containing an expanded polyglutamine repeat is associated with oxidative stress and toxicity in striatal neurons. Nuclear factor erythroid 2-related factor 2 (Nrf2) is a redox-sensitive transcription factor responsible for regulating expression of a diverse array of antioxidant and cytoprotective genes. Most known Nrf2-activating compounds act through the canonical pathway by mimicking a transient oxidative insult, and treatment effects are short-lived. This study reveals an increase in striatal cell viability, and a reduction in mitochondrial reactive oxygen species (ROS) levels, following treatment with the non-canonical Nrf2-activator 2,3-dimercaptopropanol (DMP). DMP was also found to prevent the formation of Keap1- and Nrf2-positive inclusion bodies. The current study highlights previously unknown intracellular targets of DMP and indicates that this FDA approved compound may have relevance for the treatment of HD and other neurodegenerative disorders.

Keywords: Huntington's disease, HD, antioxidant, ROS, DMP, BAL

Acknowledgments

I would like to express my deepest gratitude to Dr. Robert Cumming for the ongoing mentorship and guidance throughout the entirety of my project over the last two years. I am incredibly grateful for his patience in personally teaching me many of the scientific methods used in this investigation, as well as providing me with an amazing atmosphere for doing research. In addition, I would like to thank my committee members, Dr. Martin Duennwald and Dr. Patrick Lajoie, for their invaluable insight, and for helping to provide direction for my project during some of the more difficult times. I would also like to extend thanks to the Huntington Society of Canada for providing the funding for my project.

I am also very grateful to the past and present fellow members of the Cumming Lab, for their unwavering support and encouragement. Many thanks go out to Richard Harris, Asad Lone, and Tyler Tam, for their friendship and advice; it would have been a lonely lab without them. A special thanks to our lab technician, Chunhui Li, whose enthusiasm for scientific research was a great source of inspiration. Additionally, I would like to thank Dr. Jordan Newington for introducing me to such an amazing group of people.

Finally, I would like to thank my parents, Linda and Graeme, and my sister, Courtney, who have always believed in me and supported me unconditionally. I would also like to thank Chris Pulford, for always being there for me.

Table of Contents

List of Abbreviations

3-NP	3-Nitropropionic Acid
ARE	Antioxidant Response Element
CRM1	Chromosome Region Maintenance 1
Cul3	Cullin-3
DMP	2,3-Dimercaptopropanol
DPBS	Dulbecco's Phosphate Buffered Saline
ETC	Electron Transport Chain
FBS	Fetal Bovine Serum
GABA	Gamma-aminobutyric Acid
GAPDH	Glyceraldehyde 3-Phosphate Dehydrogenase
H3	Histone H3
HD	Huntington's Disease
HTT	Human Huntingtin Gene
HTT	Human Huntingtin Protein
kDa	Kilo Dalton
Keap1	Kelch-Like ECH-Associated Protein 1
LMB	Leptomycin B
mHTT	Mutant Huntingtin Protein
MSNs	Medium Spiny Neurons
MTT	3-(4,5-Dimethylthiazol-2-yl)-2,5-Diphenyltetrazolium Bromide
Nrf2	Nuclear Factor Erythroid 2-Related Factor 2
PAGE	Polyacrylamide Gel Electrophoresis
PMSF	Phenylmethansulfonylfluoride
PolyQ	Polyglutamine

Prx-1	Peroxiredoxin-1
PVDF	Polyvinylidene Fluoride
ROS	Reactive Oxygen Species
SDS	Sodium Dodecyl Sulfate
SFN	Sulforaphane
tBHQ	*Tert*-Butylhydroquinone
TBS-T	Tris Buffered Saline with Tween 20
Ub	Ubiquitin
WT	Wild-type

List of Figures

Chapter 1 : Introduction

1.1 Huntington's Disease Overview

Huntington's disease (HD) is a fatal, progressive neurological disorder characterized by mid-life onset and gradual worsening of motor dysfunction, emotional disturbances, and cognitive decline, with death occurring 15-20 years from onset. The disease was named after George Huntington, the American doctor who described a patient with classical symptoms of the condition in 1872 (Huntington, 1872). HD affects roughly 1 in every 7,000 Canadians (Huntington Society of Canada, 2014), and 5-10 individuals per 100,000 worldwide, making it the most common inherited neurodegenerative disorder (Landles and Bates, 2004). The disease is caused by a dominantly inherited CAG trinucleotide repeat expansion in the HD gene (*HTT*) encoding the multi-functional huntingtin protein (HTT). The expansion results in an extended polyglutamine domain that promotes protein misfolding and causes neuronal cell death in a number of brain regions. Although HD is a monogenic disease, symptom onset and progression appears to be relatively variable among affected individuals (Kirkwood et al., 2001). A number of studies have reported that age at onset decreases and disease severity increases with increasing lengths of the CAG repeat (Andrew et al., 1993; Claes et al., 1995; Ruocco et al., 2006). Although HD most commonly manifests during the third to fifth decades of life, studies have revealed that the age of onset follows an essentially normal distribution. Surveys have shown that approximately 5-10% of cases are juvenile-onset and present in persons less than 20 years of age, and even fewer cases present after the age of 60 (Ribaï et al. 2007; Lipe & Bird, 2009; Nance & Myers, 2001). Patients with adult-onset HD, which represents the majority of cases, typically develop mood imbalances, such as depression and irritability, prior to the onset of movement disorders (Duff et al., 2007). Nevertheless, the definitive clinical feature of HD is chorea: a hyperkinesia characterized by abrupt, unpredictable, involuntary movements that, in early HD, makes the patient appear clumsy or fidgety. However, as the involuntary movements increase in frequency and amplitude they begin to interfere with normal speech, swallowing, posture, and gait. Moreover, HD patients

have an increased risk of skin injuries, infections, bone fractures and even head trauma in the mid to late stages of the disease. In the end stages of the disease, patients develop dystonic postures, rigidity, and full dementia (Di Maio et al., 1993). Due to the widespread expression of the affected protein, HD patients also exhibit abnormalities in peripheral tissues, such as muscle atrophy and dramatic weight loss (Sanberg et al., 1981; Trejo et al., 2004). The leading causes of death arise from complications associated with immobility, such as pneumonia, cardiac disease, and infection. However, due to the progressive loss of behavioural control and cognitive ability, suicide risk is much higher in HD patients, and accounts for almost 10% of patient deaths (Baliko et al., 2004; Di Maio et al., 1993 Heemskerk & Roos, 2010).

The pathological hallmark of HD is the striking degeneration of the caudate nucleus and the putamen, together known as the striatum (Ruocco et al., 2006). The GABAergic medium spiny projection neurons (MSNs) constitute the majority of neurons in the striatum and appear to be particularly susceptible to the toxicity associated with mutant huntingtin protein (mHTT) expression. MSNs receive excitatory input from the entire cerebral cortex and thalamus, and provide an inhibitory output to areas of the brain that are involved in the regulation of voluntary movement, such as the globus pallidus and the substantia nigra pars reticulata. This loss of inhibitory innervation is thought to be the cause of chorea in early to mid-stage HD. Additionally, there is substantial cortical neuron cell death, severe loss of subcortical white matter, and enlargement of the ventricles (Suzanne, Vonsattel & Richardson, 1988). The collective neuropathologies associated with HD give the appearance of a shrinking brain; by the late stages of HD an afflicted brain can weigh 20-30% less than a healthy brain, depending on the severity of the disease (Vonsattel & DiFiglia, 1998).

There is currently no cure for HD, and the current drug therapies possess no ability to delay the onset or slow the progression of the disease. Pharmacotherapies typically used to manage the movement disorders of HD act by rebalancing the neurotransmitters in the basal ganglia (Erdemoglu and Boratav, 2002). However, these medications have limited utility due to a number of worrisome side effects, such as Parkinsonism, loss of balance, and dysphagia, as well as an exacerbation of a number of psychiatric symptoms, such as

depression. Several psychiatric disturbances also respond well to pharmacological intervention; most commonly patients are prescribed antidepressants and anti-psychotics with a variety of mechanisms of action (Erdemoglu and Boratav, 2002; Ford, 1986). Patients receive a drug regimen tailored to their particular constellation of movement and psychiatric symptoms; however, in many cases, the efficacies of pharmacological intervention are modest, and the behavioural symptoms associated with the disease make noncompliance a prevalent issue in symptomatically treating HD patients (Armstrong et al., 2012; Bonelli and Hofmann, 2007). In light of this, there has been a shift in research focus toward the development of neuroprotective treatment strategies. This approach is beneficial in that it has the potential to slow or halt disease progression. Several studies have looked at agents that confer neuroprotection by disrupting the transcription of mHTT (Ryu et al., 2005), or interfering with harmful mHTT-protein interactions (Bauer et al., 2010; Li and Li, 2004; Slow et al., 2006). More general neuroprotective agents, such as apoptosis inhibitors (Chen et al., 2000) and drugs that upregulate transcription of cytoprotective or antioxidant genes (Huntington Study Group, 2001; Ranen et al., 1996), have shown promise; however, much more research needs to be done.

1.2 Molecular Basis for HD

The gene responsible for HD (*HTT*) was molecularly mapped to the short arm of human chromosome four in 1983 (Gusella et al., 1983), and the nature of the causative mutation was teased out nearly a decade later (MacDonald et al., 1993). The HD gene encodes a multi-functional, 350kDa protein called huntingtin (HTT), which is ubiquitously expressed throughout the central nervous system, in peripheral tissues, and during embryonic development (Bhide et al., 1996; Strong et al., 1993). The HD mutation comprises an unstable DNA segment caused by a polymorphic expansion of the $(CAG)_n$ repeat within exon 1 of the HD gene. The resultant expansion in the number of glutamine residues in the polyglutamine (polyQ) repeat region of the huntingtin protein is predictive of both the age of onset and the severity of the disease (MacDonald et al., 1993). The expanded polyglutamine region makes the mutant huntingtin protein (mHTT) highly susceptible to misfolding and aggregation, which is thought to lead to the formation of

toxic intracellular inclusion bodies (Landles and Bates, 2004). This susceptibility rises with increasing CAG repeat lengths: *HTT* alleles within the range $(CAG)_{6-35}$ are non-pathogenic and result in a normal phenotype, whereas individuals possessing alleles within the range $(CAG)_{36-39}$ are only at an increasing risk of developing the disease, and alleles with $(CAG)_{40}$ or higher are associated with fully penetrant HD. Approximately 5-7% of afflicted individuals possess alleles of $(CAG)_{70}$ or higher and present with juvenile-onset HD (Nance and Myers, 2001).

Wildtype huntingtin (wt HTT) is mostly cytoplasmic, with a small intranuclear portion. The complete repertoire of HTT cellular functions is still not clearly defined because it contains little sequence homology to other known proteins (MacDonald et al., 1993). One important region in the protein is the polyQ region; it begins at the eighteenth amino acid from the NH_2-terminus and forms a polar zipper structure, which functions to bind transcription factors that also contain a polyQ stretch (Li and Li, 2004; Perutz et al., 1994). Downstream from this, HTT contains multiple HEAT (Huntingtin, Elongation factor 3, protein phosphatase 2A, and the lipid kinase TOR) repeat sequences. HEAT repeats are 30-40 amino acid motifs comprised of two anti-parallel α-helices. These motifs often assemble into superhelical structures with continuous hydrophobic cores (Andrade and Bork, 1995), which indicates that HTT may play a scaffolding role in facilitating protein-protein interactions. Huntingtin also contains functionally active nuclear export/localization signals at the carboxy terminus, implicating the protein in nuclear-cytoplasmic transportation (Xia et al., 2003). Some of these roles include clathrin-mediated transport of endocytic and secretory vesicles (Velier et al., 1998), and interacting with huntingtin-interacting proteins (HIPs) and huntingtin-associated proteins (HAPs; Neuwald & Hirano, 2000; Takano and Gusella, 2002).

The necessity of HTT during different stages of development is demonstrated by a number of studies that experimentally reduced the wildtype protein levels. Embryonic lethality occurs prior to gastrulation and formation of the nervous system in huntingtin-knockout mice ($Hdh^{-/-}$; Zeitlin, et al., 1995). Additionally, heterozygote ($Hdh^{+/-}$) and *Hdh*-knockdown (<50%) studies suggest that, following gastrulation, normal levels of wildtype HTT become essential for proper neurogenesis and formation of the cortex and

striatum (Nasir et al., 1995; White et al., 1997). Interestingly, during development the expression of mHTT can compensate for the absence of wildtype huntingtin (Leavitt et al., 2001), and individuals that are homozygous for mHTT are born without neurological defects (Wexler et al., 1987). This indicates that, during development, the HD mutation does not interfere with the function of normal huntingtin, and does not confer a toxic gain-of-function. Furthermore, patients possessing just a single fully functional huntingtin allele do not develop HD, which provides evidence that the disease is not exclusively caused by the loss of huntingtin function (Ambrose et al., 1994).

In post-mitotic brain cells and adulthood, the altered protein structure that results from the polyQ expansion gives rise to aberrant protein interactions that cause cytotoxicity and simultaneously interfere with normal huntingtin function. Wildtype (wt) HTT, but not mHTT, also plays a critical role in the transcriptional regulation (Zuccato et al., 2001) and anterograde transportation of brain-derived neurotrophic factor (BDNF) from cortical cells to the striatum, where it provides neurotrophic support for striatal cell survival and maintains the integrity of the cortico-striatal synapses (Gauthier et al., 2004). The presence of mHTT or a decrease in the levels of wt HTT both drastically reduce the striatal levels of BDNF and may partially account for the increased susceptibility of medium spiny neurons in HD (Zuccato et al., 2001; del Toro et al., 2006). Interestingly, the function of huntingtin as an effective transport molecule seems to hinge upon post-translational modifications, which are disturbed in mHTT (Zala et al., 2008). The polyQ expansion in mHTT impairs its nuclear export capabilities (Cornett et al., 2005). A number of studies have shown that HTT has anti-apoptotic properties: *in vitro* studies of conditionally-immortalized striatal cells over-expressing the human wildtype protein have shown that wt HTT exerts its protective effects by preventing the activation of caspase-3, possibly at the level of caspase-9 (Rigamonti et al., 2000). Moreover, overexpression of wt HTT confers gene dose-dependent neuroprotection against ischaemic injury *in vivo* (Zhang et al., 2003), excitotoxicity (Leavitt et al., 2006), and is also able to alleviate the harmful effects of the mutant protein (Rigamonti et al., 2001), which suggests that the HD neuropathology can likely be partially attributed to a loss of the wildtype huntingtin function.

The mutant huntingtin protein also bears a toxic gain-of-function, which is commonly attributed to its propensity for novel protein-protein interactions and aggregation into fibrillar strands, which ultimately form large intracellular inclusion bodies (Butterfield & Kanksi, 2001). The production of cytotoxic HTT fragments is a central component of HD pathogenesis. The N-terminal region of HTT is a common cleavage site for a number of proteases, and in vitro studies have revealed that the polyQ expansion observed in HD enhances the cytotoxicity of proteolytically cleaved HTT (Hackam et al., 1998). Indeed, the intracellular, and often nuclear, accumulation of N-terminal mHTT fragments is a neuropathological hallmark of HD (Hackam et al., 1998). In a mouse model of HD that expresses the full-length mutant huntingtin protein, researchers found that the nuclear localization of huntingtin fragments occurred first and most drastically in the striatum, which could account for the regional sensitivity in the disease (Van Raamsdonk et al., 2005). Further studies revealed that the same mice now expressing a caspase-6-resistant version of mHTT do not develop striatal neurodegeneration, and are actually protected against stressor-induced neurotoxicity (Graham et al., 2006). Following cleavage by caspase-6, transglutaminases catalyze the covalent cross-linking of mHTT N-terminal fragments to form cytotoxic oligomers. These oligomers increase in number within the cytoplasm until they reach a threshold concentration, at which point a nucleation event occurs, triggering the formation of inclusion bodies (Ossato et al., 2010; Zainelli et al., 2005). Aggregates of mHTT have been reported to act as physical roadblocks impairing mitochondrial movement (Chang et al., 2006), and mHTT oligomers directly interfere with microtubule-associated axonal transport by binding key motor proteins. This may contribute to the enhanced susceptibility of the MSNs in the striatum due to their extensive dendritic branching (Trushina et al., 2004).

1.3 Oxidative Stress in HD Neurodegeneration

Redox homeostasis is essential for proper neuronal function and its perturbation, resulting in oxidative stress, is often implicated in triggering cell death pathways in neurodegenerative diseases associated with protein aggregates, including HD (Martínez et al., 2010). The redox state of a cell is defined by its ability to balance the production of

reactive oxygen species (ROS) with its antioxidant defense capacity. ROS are unstable, oxygen-containing molecules that are generated by the sequential reduction of oxygen during a number of normal cell processes. They exhibit profound reactivity due to the unpaired electron in the valence shell of oxygen (Dasuri et al., 2013). Although there are numerous intracellular sources of ROS, oxidative phosphorylation associated with mitochondrial electron transport chain (ETC) activity is a major source of the superoxide radical ($O_2^{\bullet}$), which is a precursor for many other reactive species, including hydrogen peroxide (H_2O_2), and the more reactive hydroxyl radical ($OH^{\bullet}$; Guidot et al., 1993). The function of the ETC is to produce useful chemical energy by passing electrons along a chain of molecules, in which oxygen is the terminal acceptor. Under basal conditions, a small percentage of the electrons leak out of the ETC and interact with oxygen to form ROS, which, at normal physiological levels, maintain cell homeostasis and function as important second messengers in cell signaling by extracting electrons from neighbouring macromolecules, thereby modifying their biological functions (Sena & Chandel, 2012; Valko et al., 2004). Proteins containing cysteine residues within their functional domains are highly sensitive to ROS-mediated modification; oxidation of the sulfhydryl groups (Cys-SH) can promote the formation of intra-protein disulfide linkages (Cys-S-S-Cys) thereby altering protein function or interactions with other proteins (Cumming et al., 2004).

Oxidative stress occurs when there is an excessive production of reactive oxygen species (ROS), inadequate antioxidant defense capacity, or both, which results in subsequent cellular damage. When ROS accumulate to high concentrations within the cell, extensive oxidative damage can impair the normal function of cell components, thereby promoting disease states. It has been well established that oxidative stress is involved in the pathogenesis of a number of neurodegenerative diseases, including Alzheimer's, Parkinson's and Huntington's diseases. Because age is a risk factor in theses diseases, and we know that ROS increase in the brain with age, we can postulate that ROS plays a role in pathological neurodegeneration (Mariani et al., 2005). Unwarranted protein oxidation can result in aberrant protein functions and structure, and can also cause fragmentation (Berlett & Stadtman, 1997). Oxidation tends to increase the protein's hydrophobicity, which may induce protective proteolysis; however, it can also promote

protein aggregation (Dasuri et al., 2010; Shringarpure et al., 2001). The brain is especially susceptible to oxidative stress due to the elevated levels of oxygen consumption and high polyunsaturated fatty acid content. Peroxidation of phospholipids compromises the structural integrity of the cell membrane and triggers detrimental free radical chain reactions, which produce intermediates that form harmful adducts with DNA (Bartsch, 1997; Porter, 1986). Interestingly, elevated lipid peroxidation products have been reported in the striatum of huntingtin-overexpressing transgenic mice, as well as in the cerebrospinal fluid of HD patients (Perez-Severiano et al., 2000; Montine et al., 1999). Additionally, direct oxidative damage to nucleic acids in DNA promote mutagenesis, further implicating oxidative stress in the development of age-dependent diseases such as cancer and neurodegenerative disorders (Ames et al., 1994; Valko et al., 2004). Mitochondrial DNA is particularly vulnerable to oxidative damage as a result of being a major ROS generator coupled with inferior DNA repair mechanisms (Lin & Beal, 2006). A number of studies have provided supporting evidence for a link between mitochondrial dysfunction and oxidative damage in early and late-stage HD patients, as well as in animal and cell culture models of HD (Brown & Beal, 2006). Succinate dehydrogenase (SDH), or respiratory complex II, is a functional member of both the mitochondrial electron transport chain, and the citric acid cycle. Prolonged systemic administration of 3-nitropropionic acid (3-NP), an irreversible mitochondrial complex II inhibitor, to animals induces targeted oxidative stress and neurodegeneration in the striatum by damaging cell metabolism, which results in a reduction in ATP production. This causes striatal lesions and gait abnormalities that mimic HD (Beal et al., 1993; Brouillet et al., 1995). Furthermore, mitochondria isolated from a transgenic mouse model of HD demonstrate reduced membrane potential and heightened sensitivity to calcium-induced release of cytochrome *c* when compared with controls (Panov et al., 2002). This supports the hypothesis that increased oxidative stress seen in neurodegenerative diseases confers an increased susceptibility for programmed cell death.

1.4 Activation of Nrf2 and the Antioxidant Response

Following the discovery that elevated oxidative stress contributes to these neurodegenerative diseases, researchers proposed the therapeutic administration of exogenous antioxidants; however, these treatments did not produce favourable results. The majority of exogenous antioxidants are hydrophilic and therefore unable to effectively cross the blood-brain barrier. This, coupled with their toxicity at high doses makes their therapeutic efficacy quite low (Moosmann & Behl, 2002). In an effort to more effectively restore redox homeostasis, researchers shifted their target to increasing expression of endogenous antioxidant enzymes already present in the central nervous system (Schreibelt et al., 2007). A number of these protective genes conveniently share a common promotor region, known as the Antioxidant Response Element (ARE), which is regulated by the transcription factor, Nuclear factor (erythroid-derived 2)-like 2 (Nrf2; Kensler et al., 2007). ARE target genes include the antioxidant peroxiredoxin-1 (PRX1) as well as the phase II detoxifying enzymes, such as glutathione-S-transferase (GST) and heme oxygenase (HO; He & Ma, 2010). Nrf2 is the regulatory transcription factor that modulates the expression of several antioxidant and cytoprotective genes in order to maintain and restore redox homeostasis. Under basal conditions (Figure 1, top) Nrf2 is constitutively expressed but is maintained at very low levels because it is bound in the cytoplasm by its negative regulator, Kelch like-ECH-associated protein 1 (Keap1). Keap1 binds Nrf2 in the cytoplasm and forms an E3 ubiquitin ligase complex with Cullin-3 (Cul3) in order to poly-ubiquitinate and subsequently degrade Nrf2 via the 26S proteasome (Villeneuve et al., 2010). The interaction between Nrf2 and Keap1 is thought to behave like an intracellular sensor of oxidative stress due to its proclivity for dissociation in the presence of reactive oxygen species and/or electrophiles (Koboyashi et al., 2004). Following the oxidation of critical cysteine residues, Keap1 undergoes a conformational change, which causes Nrf2 and Keap1 to detach from the ubiquitin-ligase complex. This dissociation allows for the stabilization and translocation of Nrf2 into the nucleus where it dimerizes with small musculoaponeurotic fibrosarcoma oncogene homolog (Maf) proteins in order to bind to the cis-acting ARE and up-regulate the transcription of a battery of antioxidant and cytoprotective genes (Itoh et al., 2003). Additionally, experimental overexpression of Nrf2 was found to be protective against

oxidative stress induced by the mitochondrial complex II inhibitor 3-NP both in vivo and in vitro (Calkins et al., 2005). The increased expression of these free radical scavenging enzymes, which convert toxic ROS to water, comprise a powerful antioxidant defense against oxidative damage.

A number of known canonical Nrf2-activators act by mimicking a transient oxidative insult by promoting the dissociation of Nrf2 from the Keap1-Cul3 complex (Figure 1, left), which causes a subsequent increased expression of key antioxidant proteins (Nguyen et al., 2004). Indeed there is substantial evidence to support a protective role of Nrf2-induced antioxidant defense in neurodegeneration. Both *tert*-butylhydroquinone (tBHQ) and sulforaphane (SFN), which are canonical Nrf2 activators, were protective against oxidative stress, neurodegeneration and cerebral ischemia *in vivo* (Shih et al., 2005; Zhao et al., 2006). More recently, SFN was found to suppress the formation of a lesion area, reduce neuronal death, rescue the decrease in succinate dehydrogenase activity, and reduce the levels of inflammatory mediators in the striatum of a 3-NP-induced mouse model of HD (Jang and Cho, 2015). Given that there exists a well-established role of oxidative stress in neurodegenerative diseases such as HD, therapeutics that aim to increase the endogenous antioxidant defense systems by enhancing the transcriptional activity of Nrf2 could hypothetically slow disease progression by increasing the lifespan of affected neurons. Interestingly, an alternative, or non-canonical, mechanism of Nrf2 activation has been discovered, which involves the formation of covalent adducts between Keap1 and the electrophile, such as arsenic, followed by the subsequent autophagosomal degradation of Keap1 (Lau et al., 2010; Lau et al., 2013). Non-canonical activation of Nrf2 operates through the p62/SQSTM1 (sequestosome 1) protein, which is a selective substrate adapter protein that plays a critical role in the autophagy process due to its ability to bind both ubiquitinated proteins as well as the autophagosome-localizing protein, LC3 (Pankiv et al., 2007). Thus p62 can selectively direct Keap1 towards autophagosomal degradation, thereby allowing the stabilization and nuclear translocation of Nrf2. To date, the differential protection conferred by canonical or non-canonical Nrf2 activators for the treatment of HD has not yet been explored; however, a recent study suggests that non-canonical activators, such as

2,3-dimercaptopropanol (DMP) may elicit a potent and prolonged activation of Nrf2 (Pitts et al., 2012).

1.5 2,3-Dimercaptopropanol

2,3-Dimercaptopropanol (DMP), also known as British anti-lewisite (BAL), is a heavy metal-chelating dithiol compound that was developed in 1940 as an antidote to the arsenic-based chemical warfare agent lewisite (Waters & Stock, 1945). Arsenic and other heavy metals form complexes with and inactivate sulfhydryl-containing proteins and enzymes. One such enzyme, pyruvate dehydrogenase, is essential for pyruvate metabolism, and its inhibition leads to lactic acidosis and cell death (Petrick et al., 2001). DMP is more stable than naturally occuring dithiols, and because heavy metals prefer to form complexes with stable thiol complexes, treatment with DMP reverses the inhibition of these essential enzymes, thereby ameliorating their toxic effects (Vilensky & Redman, 2003). In 1951 DMP was successfully used to treat patients with hepatolenticular degeneration resulting from copper accumulation in the liver (Denny-Brown & Porter, 1951). At this time, HD was thought to be caused by copper accumulation in the brain (Vilensky & Redman, 2003) and DMP was administered daily to two HD patients over the course of a year (Nielsen and Butt, 1955: Appendix: Figure III). In both cases DMP was shown to attenuate disease progression; however, the study was discontinued due to the extensive formation of abscesses at the intramuscular injection sites and was abandoned as a therapy due to inconsistencies with the theory of copper-induced HD (Campbell et al., 1961). Today, DMP is still indicated for the treatment of heavy metal poisoning, especially with arsenic, gold, mercury, and lead (Vilensky & Redman, 2003). In a recent cell-based screen for FDA-approved compounds to treat Huntington's disease, DMP was found to elicit the highest degree of neuroprotection against mutant huntingtin (mHTT)-induced toxicity (Aiken & Schweitzer, 2004). Upon further experimentation, researchers found that DMP is a potent activator of Nrf2 (Pitts et al., 2012), which suggests that the neuroprotective effects of DMP are derived, in part, from its ability to elicit an intracellular antioxidant response. Interestingly, a previous study found that DMP binds the same cysteine thiols in Keap1 as arsenic does (He & Ma, 2010). Several

studies have shown that arsenic activates Nrf2 through the non-canonical mechanism by promoting the autophagosomal degradation of Keap1 (Lau et al., 2013). This suggests that DMP may be working via the non-canonical pathway (Figure 1, right). However, it is still uncertain if DMP exerts its neuroprotective effects against mHTT-induced toxicity exclusively by Nrf2 activation.

1.6 Hypothesis and Research Outline

The expression of mHTT has been shown to exacerbate intracellular oxidative stress by interfering with Nrf2-dependent ARE-directed expression of cytoprotective genes in a PC12 cell line capable of inducible expression of mHTT (Dailey, 2012). In addition, DMP was found to be neuroprotective through the induction of Nrf2 activity and the subsequent upregulation of cytoprotective and antioxidant genes (i.e., Prx1; Dailey, 2012; Pitts et al., 2012). In this study it is hypothesized that the neuroprotective effects of DMP are mediated via non-canonical Nrf2 activation. Experiments will be performed using more clinically-relevant striatal cell lines derived from a knock-in transgenic mouse expressing humanized Exon 1 of HTT with either 7 ($STHdh^{Q7}$) or 111 ($STHdh^{Q111}$) poly-glutamine repeats, which will serve as wild-type and HD cell lines, respectively. The mechanisms by which DMP exerts its effects will be examined by looking at changes in whole cell protein levels, as well as the subcellular localization of key proteins: Nrf2, Keap1, and p62.

Figure 1

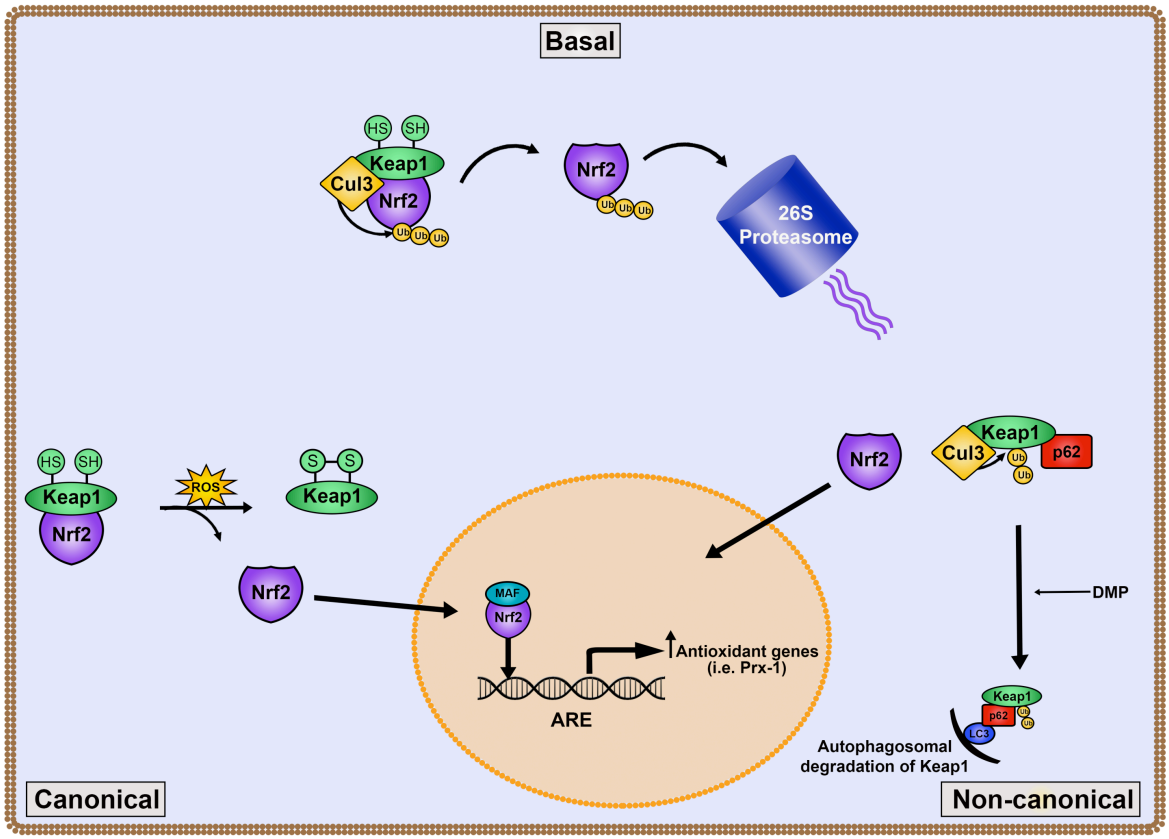

Figure 1. Proposed mechanism by which DMP promotes non-canonical activation of Nrf2. Under basal cell conditions, Nrf2 is sequestered in the cytosol by its negative regulator, Keap1, which forms a Cul3-dependent E3 ubiquitin ligase complex to facilitate the poly-ubiquitynation and subsequent degradation via the 26S proteasome (top). Canonical activation of Nrf2 occurs when ROS-triggered oxidation of thiol groups in Keap1 promotes a conformational change resulting in the release of Nrf2. Nrf2 is no longer targeted for proteasomal degradation and is then free to enter the nucleus where it can bind to antioxidant response elements (AREs) and promote increased transcription of antioxidant and cytoprotective genes (left). In the non-canonical pathway, Keap1 binds to p62 and is targeted for degradation by the autophagosomal system, thereby releasing Nrf2, which translocates into the nucleus. DMP may promote increased interaction between Keap1 and p62, or help facilitate the targeting of these proteins to emerging autophagosomes (right).

Chapter 2 : Materials and Methods

2.1 Cell Culture

The experiments outlined in this study were performed in two immortalized striatal cell lines derived from a knock-in transgenic mouse containing homozygous *Huntingtin* (HTT) loci with a humanized Exon 1 with either 7 ($STHdh^{Q7}$) or 111 ($STHdh^{Q111}$) poly-glutamine repeats. These two cell lines are representative of a wildtype or HD-afflicted phenotype, respectively. Cells were incubated at 33°C and 5% CO_2 and were maintained in high glucose/high serum media (HH media: Dulbecco's Modified Eagle Medium (DMEM) containing 4.5g/L glucose and supplemented with 5% fetal bovine serum (FBS) and 1% penicillin/streptomycin). During drug treatment studies the cells were cultured in low/low media (LL media: DMEM containing 1g/L glucose and supplemented with 1% FBS and 1% penicillin/streptomycin) to ensure that the potentially protective effects of the serum metabolites did not confound the results. Due to the ability of $STHdh^{Q111}$ cells to survive and proliferate in the presence of mHTT, both cell lines were stressed with the mitochondrial complex II inhibitor, 3-NP, in order to assess the protective effects of DMP.

Later experiments were also performed on mouse hippocampal HT22 cells, which served as the transfection-tolerant cell line. HT22 cells were incubated at 37°C and 5% CO_2 and were maintained in DMEM containing 4.5g/L glucose and supplemented with 10% FBS, and 1% penicillin/streptomycin.

2.2 Subcellular Fractionation and Immunoblot Analysis

For nuclear fractionation, cells were rinsed with 1x Dulbecco's Phosphate Buffered Saline (DPBS), trypsinized with TrypLE™ Express Enzyme and centrifuged at 1.5 rpm for 5 minutes. The supernatant was discarded and cells were resuspended in hypotonic lysis buffer (20mM Tris (pH 7.4), 10mM NaCl, 3mM $MgCl_2$, 1mM PMSF, protease

inhibitor) and incubated on ice for 15 minutes. Cells were then lysed using 10% NP-40 in $_dH_2O$, and centrifuged at 4°C at 6000g for 5 minutes. The cytosolic fraction (supernatant) was transferred to another vial. The nuclear pellet was rinsed twice in hypotonic lysis buffer containing 1% NP-40 and then resuspended in SDS lysis buffer (50mM Tris (pH 7.5), 2% SDS, 1mM PMSF, protease inhibitors) and sonicated. Harvested protein concentrations were quantified by Lowry assay using a colourimetric DC™ Protein Assay Kit (BioRad). Protein extracts were then reduced in loading buffer containing 100mM dithiothreitol (DTT) and 2% β-mercaptoethanol (BME) and boiled for 5 minutes. The samples were resolved by SDS-PAGE on a 12% polyacrylamide gel using a Mini-PROTEAN® gel electrophoresis apparatus, and transferred onto a polyvinylidine fluoride (PVDF) membrane via electroblotting overnight at 4°C. The PVDF membrane was rinsed in Tris-buffered saline containing 1% Tween-20 (TBS-T), incubated in blocking solution (TBS-T + 3% bovine serum albumin, 1% milk powder) for a minimum of one hour at room temperature, rinsed again with TBS-T, and then probed with a primary antibody overnight at 4°C. The following primary antibodies were used for immunoblot analysis in this study: polyclonal rabbit anti-Nrf2 (Santa Cruz Biotechnology), polyclonal rabbit anti-Keap1 (ProteinTech), polyclonal rabbit anti-Prx-1 (AbFrontier), polyclonal rabbit anti-p62 (Cell Signaling), polyclonal rabbit anti-GAPDH (IMGENEX), and polyclonal rabbit anti-Histone H3 (Cell Signaling Technology),

The following day, PVDF membranes were rinsed with TBS-T and incubated in blocking solution containing the appropriate secondary antibody (1:10000 dilution) at room temperature for one hour. The following secondary antibodies were used for immunoblot analysis in this study: blotting grade goat anti-rabbit IgG (H+L) Horseradish Peroxidase Conjugate 170-6515 (BioRad, Hercules, CA, USA) and blotting grade goat anti-mouse IgG (H+L) Horseradish Peroxidase Conjugate 170-6516 (BioRad, Hercules, CA, USA). Membranes were then rinsed again with TBS-T and developed using SuperSignal® West Pico Chemiluminescent Substrate (Thermo Scientific). Protein signal was detected by Molecular Imager® ChemiDoc™ XRS System (BioRad), and densitometric analyses were performed using ImageJ software. Band densities were standardized against the loading control, glyceraldehyde 3-phosphate dehydrogenase (GAPDH).

2.3 Immunofluorescence Microscopy

Glass coverslips (18mm) were autoclaved and coated with poly-D-lysine (50µg/mL) in a 12-well plate for at least 3 hours and were then rinsed with $_dH_2O$ and allowed to dry completely. Both cell lines were seeded at the same density and incubated at 33°C overnight. The following day cells were treated with vehicle, 10mM 3-NP, 10µM DMP, or both 3-NP and DMP for 24 hours. For experiments in which immunofluorescence was performed on ectopically expressed Nrf2, cells first underwent a transient transfection: in line with standard transfection protocol, 5µg of the Nrf2-Flag plasmid was added to 8µL of Lipofectamine 2000 (Invitrogen) in 1mL of Opti-MEM I transfection media (Invitrogen). This was added to both $STHdh^{Q7}$ and $STHdh^{Q111}$ cells, which were then incubated in the transfection reagents at 33°C for 6 hours. After incubation, the transfection reagents were replaced with HH media and cells were left to recover overnight at 33°C. The morning following transfection, HH media was replaced with LL media, and the cells were treated as per previously described that afternoon. Afterward 24 hours the cells were rinsed with DPBS and then fixed with 4% paraformaldehyde in DPBS for 10 minutes. They were then washed with DPBS for 5 minutes, followed by two 5-minute washes with DPBS containing 0.1% Triton-X (PBS-T). Cells were incubated in blocking solution (PBS-T + 4% goat serum) overnight at 4°C. Coverslips were then placed cell-side down on top of a 50µl drop of primary antibody in PBS-T + 3% goat serum for a minimum of 2 hours in a humidity chamber at room temperature to limit evaporation. The following primary antibodies were used for immunofluorescence staining in this study: polyclonal rabbit anti-Nrf2 (Santa Cruz Biotechnology), monoclonal mouse anti-Keap1 (ThermoFisher Scientific), polyclonal rabbit anti-Keap1 (ProteinTech), and monoclonal mouse anti-Flag (Sigma Aldrich). Following incubation they were placed back into the 12-well plate and rinsed with PBS-T, followed by a 45-minute incubation period in appropriate secondary antibody in PBS-T + 3% goat serum. The following secondary antibodies were used for immunofluorescence staining in this study: goat anti-rabbit IgG (H+L) Alexa Fluor® 647 (Life Technologies), and goat anti-mouse IgG (H+L) Alexa Fluor® 488 (Life Technologies). The coverslips were subsequently replaced into the 12-well plate, rinsed with PBS-T, mounted onto glass slides using ProLong® Gold Antifade Reagent with the nuclear stain 4',6-Diamidino-2-

phenylindole (DAPI), and sealed with nail polish. Slides were imaged using either a Leica DM6000 M widefield fluorescent microscope or an Olympus FluoView™ FV1000 confocal microscope. Images were taken from five random locations on each slide, and exposure times were kept constant across all treatment groups. Fluorescence intensity and area values were obtained from every cell in each image using ImageJ software, and the mean values were averaged across at least three independent experiments. Statistical analyses were performed by a one-way analysis of variance (ANOVA) test, and post-hoc Tukey's test.

2.4 Trypan Blue Exclusion Test

The effects of 3-NP treatment (10mM) with or without DMP treatment (10μM) on cell viability were assessed by trypan blue exclusion test: both cell lines (STHdh Q7 and STHdh Q111) were seeded in triplicate at the same density in 12-well plates and were incubated overnight to ensure cell adherence. The following day, cells received one of the following treatments: untreated, 3-NP alone, DMP alone, or treated with DMP one hour prior to 3-NP treatment. The cells were incubated for either 24 or 48 hours following the 3-NP treatment, at which point the cell media for each well (containing detached, dead cells) was collected separately and the cells were trypsinized using 150μl of TrypLE Express and incubated at 33°C for 5 minutes. Next, cells from each well were resuspended with their respective media aliquots, placed into a 15mL conical tube, and centrifuged at 500x g for 5 minutes. Most of the supernatant was then aspirated, and the cell pellet was resuspended in 150μl of media. An equal volume of trypan blue dye was added to the cell suspension, which was then mixed and loaded into a hemocytometer for counting. Viable cells excluded the dye and appeared white, whereas dead cells took up the dye and appeared blue. Counts were performed blindly and cell viability was calculated as the number of white cells over the total number of cells counted in each sample, averaged for every treatment group. Statistical analyses were performed by a one-way analysis of variance (ANOVA) test, and post-hoc Tukey's test.

2.5 MTT Assay

To assess the influence of DMP on cytotoxicity after inducing oxidative stress, an MTT colourimetric assay was performed. NADH- or NADPH-dependent enzymes in the mitochondria of viable cells are able to reduce the yellow tetrazolium dye, MTT, to form insoluble purple formazan crystals. The crystals are subsequently dissolved in a non-polar solvent to form a coloured solution, the absorbance of which can be quantified by spectrophotometry. Because non-viable cells cannot reduce MTT to formazan, the degree of light absorption is indicative of the number of live cells. Both cell lines ($STHdh^{Q7}$ and $STHdh^{Q111}$) were cultured in LL media and were seeded in quadruplicate at the same density in 96-well plates. Cells were incubated overnight at 33°C. The next day cells received one of the following pre-treatments: media only (no treatment), or 10μM DMP. One hour after pre-treatment each plate received a treatment of either media only (no treatment) or 10mM 3-NP. At 24 and 48 hours, cells were rinsed once with 100μL of LL media to remove all traces of the treatment drugs, which might interfere with the MTT assay, and fresh LL media was added to each well. Next, 10μL of MTT solution (1mg/mL) was added to each well at a 1:10 dilution, and the plate was incubated for 3 hours (33°C, 5% CO_2). The media containing the MTT solution was then aspirated and replaced with 100μL of DMSO and the plate was left to rock overnight at room temperature. The following day absorbances were read at 570nm with a reference filter at 690nm, using the Tecan Infinite® M1000 PRO plate reader. Statistical analyses were performed by a one-way analysis of variance (ANOVA) test, and post-hoc Tukey's test.

2.6 Live/Dead Cell Viability/Toxicity Assay

The effects of 3-NP, with or without pre-treatment with DMP, on cell viability was further assessed using the LIVE/DEAD® Viability/Cytotoxicity Kit, for mammalian cells (LifeTechnologies), which utilizes the calcein AM probe to assess cell viability. Calcein AM is a fluorogenic esterase substrate that can be hydrolyzed by viable cells to a green fluorescent product (calcein); therefore the intensity of green fluorescence is correlated with the amount of cells with intact membranes and esterase activity and, thus, viability.

Both cell lines (STHdh^{Q7} and STHdh^{Q111}) were cultured in LL media and were seeded in quadruplicate at the same density in opaque-welled, glass-bottomed 96-well plates. Cells were incubated overnight at 33°C. The following day cells received one of the following pre-treatments: media only (no treatment), or 10μM DMP. One hour after pre-treatment each plate received a treatment of either media only (no treatment) or 10mM 3-NP for 24 or 48 hours. Next, media was aspirated and cells were incubated in DPBS containing calcein AM at room temperature for 40 minutes. Next, fluorescence data were obtained by exciting the florophores at 485nm and reading the emissions at 530nm using the Tecan Infinite® M1000 PRO plate reader and analyzed using Magellan™ data analysis software. Statistical analyses were performed by a one-way analysis of variance (ANOVA) test, and post-hoc Tukey's test.

2.7 Mitochondrial ROS Quantification

Mitochondrial ROS levels were visualized in both STHdh^{Q7} and STHdh^{Q111} using the fluorescent dye MitoTracker Red CM-H_2-XRos (MTR; Invitrogen). MTR is a non-fluorescent reduced dye that specifically localizes to mitochondria in live cells and fluoresces upon oxidation. An increase in fluorescence intensity is indicative of elevated mitochondrial ROS levels. Cells were seeded in LL media in 35mm plastic cell culture dishes and incubated at 33°C overnight. Then cells received one of the following pre-treatments: vehicle only (no treatment), or 10μM DMP. One hour after pre-treatment, each plate received a treatment of either vehicle only (no treatment), or 10mM 3-NP for 24 hours. Next, media was aspirated and replaced with media containing 200nM MTR and incubated at 33°C for 30 minutes. Cells were rinsed with pre-warmed DPBS and then incubated in DPBS containing 10μg/mL Hoescht stain for another 20 minutes. After this cells were rinsed twice with pre-warmed DPBS and placed in phenol red-free LL media and visualized by fluorescence microscopy (Zeiss AxioObserver, 400x magnification). Images were taken from 5 random fields of view in each plate using a Q Imaging (Retiga 1300 monochrome 10-bit) camera with Q Capture software. MTR was quantified by calculating average fluorescence intensity per unit area with ImageJ software. Statistical

analyses were performed by a one-way analysis of variance (ANOVA) test, and post-hoc Tukey's test.

2.8 Transfection of Keap1-RFP and Nrf2-GFP Vectors

STHdh^{Q7} and STHdh^{Q111} cells were seeded on a glass bottom 6-well dish, which had been previously treated with poly-D-lysine (50µg/mL) for 3 hours and then rinsed with $_dH_2O$ and allowed to dry completely. Exactly 2.5µg of Keap1-RFP and 2.5µg of Nrf2-GFP plasmids were added to 8µL of Lipofectamine 2000 (Invitrogen) in 1mL of Opti-MEM I transfection media (Invitrogen), and added to adhered striatal cells, which were then incubated in the transfection reagents at 33°C for 6 hours. After incubation, the transfection reagents were replaced with HH media and cells were left to recover overnight at 33°C. The morning following transfection, HH media was replaced with LL media, and the cells received one of the following treatments: no treatment (control), 10mM 3-NP, or 10mM 3-NP and 10µM DMP. The dish was then placed in a Chamlide stage-top incubator on a Leica DM6000 M widefield fluorescent microscope and fluorescent images were captured every 15 minutes for 6 hours using a Hamamatsu Orca digital camera equipped with Metamorph software.

HT22 cells underwent the same procedure outlined above, except that they were singly transfected with 5µg Keap1-RFP with 8µl Lipofectamine 2000.

Chapter 3 : Results

3.1 DMP confers neuroprotection against 3-NP-induced cytotoxicity in striatal cell lines expressing full-length normal and polyglutamine-expanded huntingtin

Previous studies have revealed that treatment with DMP elicits neuroprotection against cytotoxicity associated with the expression of mutant huntingtin (mHTT), likely through the activation of Nrf2 and subsequent upregulation of protective genes (i.e., Prx-1; Dailey, 2012). However, this has not been previously reported in the striatal cell lines, which express a humanized form of exon 1 of the huntingtin protein. Therefore, the first step was to assess the degree of neuroprotection elicited by DMP on striatal cells expressing either the normal or polyglutamine-expanded huntingtin protein ($STHdh^{Q7}$ and $STHdh^{Q111}$, respectively). A number of cell viability assays were performed to determine the effects of 10μM DMP on cytotoxicity induced by treatment of $STHdh^{Q7}$ and $STHdh^{Q111}$ with 10mM 3-NP for 24 and 48 hours by using the live/dead cell viability assay, MTT assay, and trypan blue exclusion assay (Figures 2A- C, respectively). Cell viability determined by the live/dead assay, which is a more sensitive test of viability, revealed a significant increase ($p < 0.05$) in viability of $STHdh^{Q7}$ at 24 and 48 hours, and $STHdh^{Q111}$ at 48 hours following pre-treatment with DMP when compared to those treated with 3-NP alone (Figure 2A). Cell viabilities determined by both MTT assay and trypan blue exclusion assay follow a similar trend; however, these results were not significant (Figures 2B, C). Due to the variability in sensitivity that occurs in these cell lines at different passage numbers, these assays may have required a larger number of replicates. DMP also appears to preserve the overall morphology and proliferative abilities of $STHdh^{Q111}$ cells, which is compromised following 3-NP treatment (Figure 2D).

Figure 2

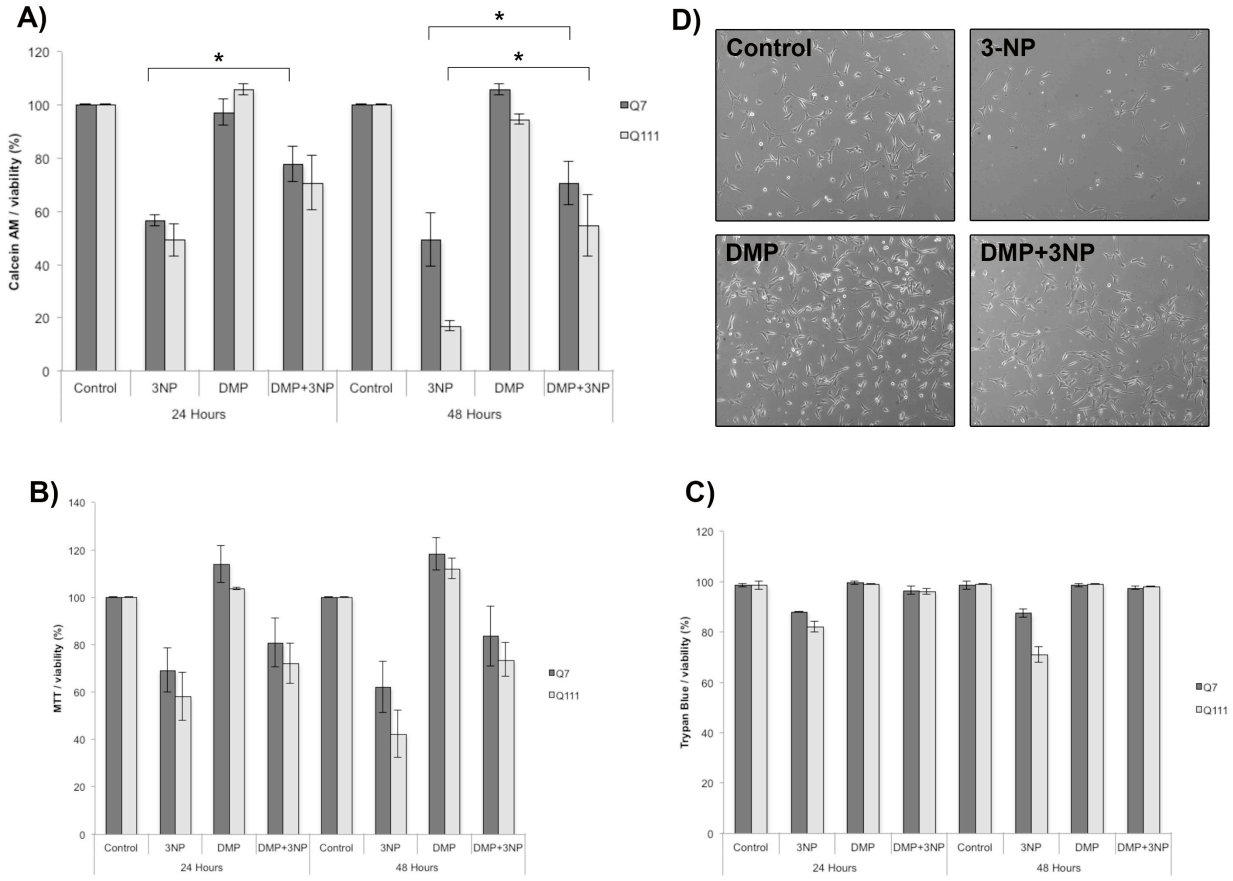

Figure 2. DMP confers neuroprotection against 3-NP-induced cytotoxicity in both STHdh^{Q7} and STHdh^{Q111} cell lines at 48 hours. Relative cell viability determined by (A) LIVE/DEAD Cell Viability® assay, (B) MTT assay, and (C) Trypan Blue assay of STHdh^{Q7} and STHdh^{Q111} cell lines grown at 33°C, treated with 10mM 3-NP and/or 10μM DMP for 24 and 48 hours. Signals obtained from the control conditions for each cell line were set as 100% viability, and the other treatment viabilities were calculated accordingly. Error bars depict standard error of the mean derived from at least three independent experiments (*, $p < 0.05$). (D) Light microscopy images of STHdh^{Q111} cells following treatment with 10mM 3-NP and/or 10μM DMP for 24 hours.

3.2 DMP treatment ameliorates the 3-NP-induced increase in mitochondrial ROS levels in STHdh^{Q111} cells

3-NP is an inhibitor of complex II in the mitochondrial electron transport chain, which leads to increased ROS production. To confirm that the cytoprotective effects of DMP are exerted through an antioxidant mechanism, mitochondrial ROS levels were assessed in live striatal cells following treatment with DMP under basal and stressed conditions. Both STHdh^{Q7} and STHdh^{Q111} were stained with MitoTracker Red CM-H_2Xros (MTR) following a 24-hour treatment with the mitochondrial toxin 3-NP with or without DMP pre-treatment. Cells were then imaged by fluorescence microscopy (400x magnification; Figure 3A). Quantification of MTR fluorescence intensity revealed a significant increase of approximately 60% ($p < 0.01$) in STHdh^{Q111} cells treated with 3-NP compared to STHdh^{Q111} cells under control conditions (Figure 7B). This was not observed in the STHdh^{Q7} cell line. Furthermore, in the STHdh^{Q111} cell line, the increase in mitochondrial ROS induced by 3-NP treatment was significantly reduced by pre-treatment with DMP ($p < 0.001$; Figure 3B).

Figure 3

A)

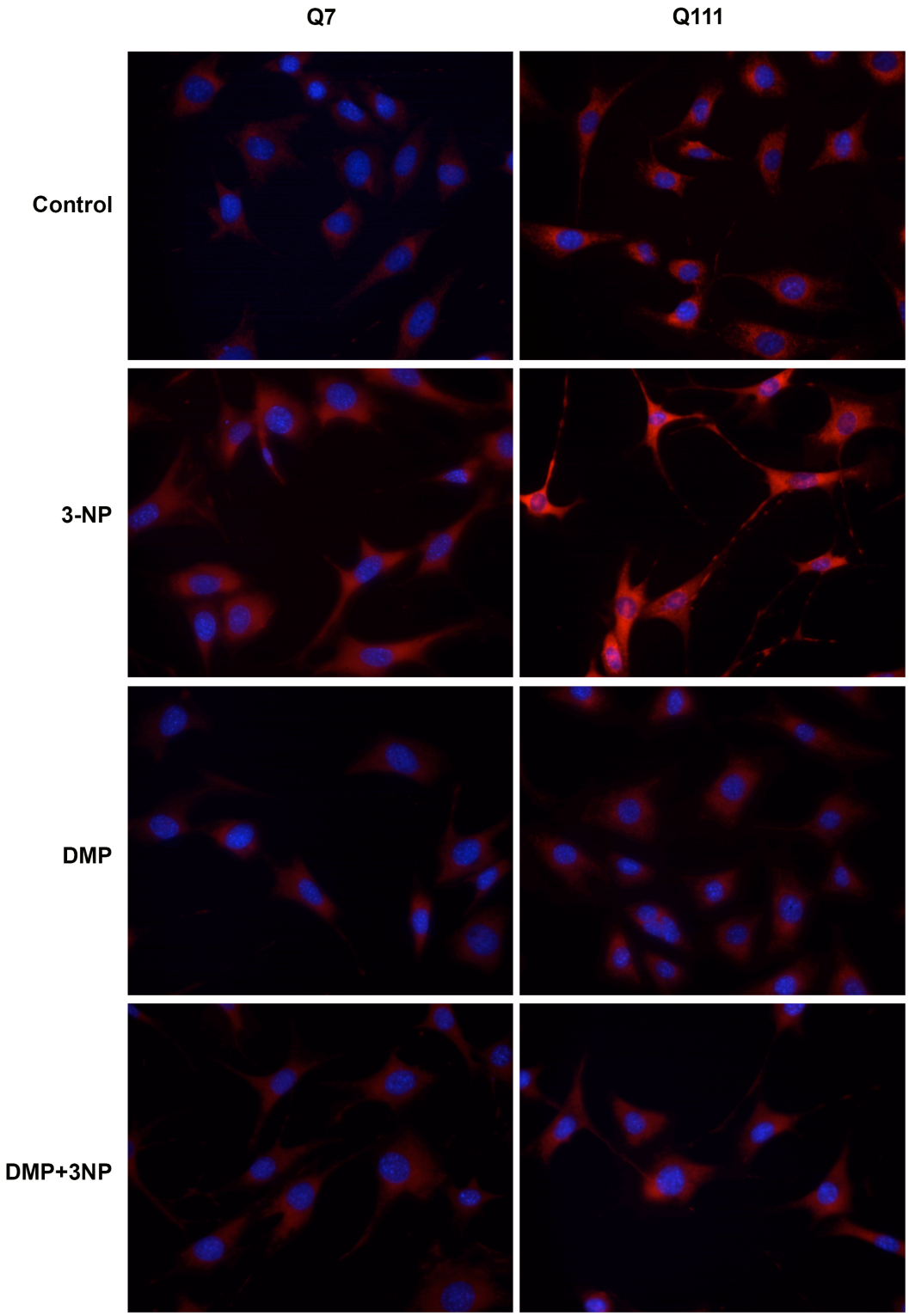

B)

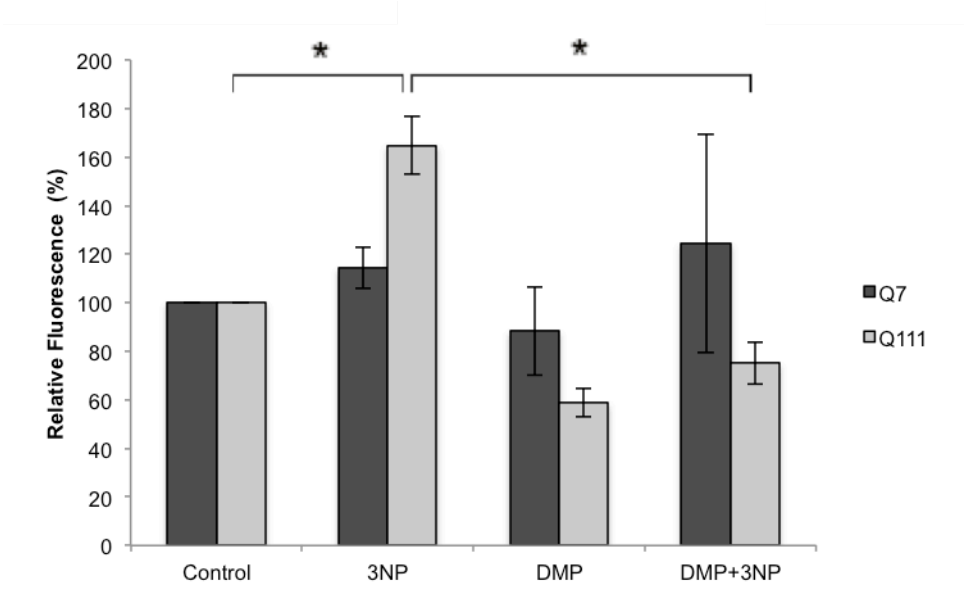

Figure 3. Pre-treatment with DMP protects against 3-NP-induced mitochondrial insult by reducing the levels of ROS in STHdh^{Q111} cells. (A) Mitochondrial reactive oxygen species (ROS) levels were measured as fluorescence intensity after staining STHdh^{Q7} and STHdh^{Q111} with the red fluorescent dye MitoTracker Red CM-H_2Xros (MTR). STHdh^{Q111} cells exhibited an elevated response to 24-hour treatment with 10mM 3-NP compared to control conditions in STHdh^{Q111} as well as 3-NP-treated STHdh^{Q7} cells. This increase was rescued by pre-treatment with 10μM DMP. Nuclei were stained blue with Hoescht and cells were observed by fluorescence microscopy at 400x magnification. **(B)** Quantification of MTR fluorescence revealed a significant decrease in STHdh^{Q111} cells that were treated with 10μM DMP prior to 3-NP treatment ($p < 0.001$). STHdh^{Q7} cells exhibited a similar trend in MTR fluorescence. Error bars represent standard error of the mean derived from three independent experiments.

3.3 DMP does not activate Nrf2 by decreasing the protein levels of its negative regulator, Keap1

In order to assess whether DMP was reducing oxidative stress by activating Nrf2 via the proposed autophagosomal degradation of Keap1, and also to determine whether DMP elicited changes in Nrf2 accumulation and downstream protein expression, whole cell lysates from STHdh^{Q7} and STHdh^{Q111} cells treated with or without 10mM 3-NP and 10μM DMP for 24 hours were analyzed by western blotting, using primary antibodies specific to Keap1, and Nrf2, as well as two downstream transcriptional targets of Nrf2: p62, and Prx-1. Antibodies specific to GAPDH were used as the loading control (Figure 4A). Contrary to what was hypothesized, neither Nrf2 nor Keap1 overall protein levels were significantly affected by treatment with DMP in either cell line (Figures 4B, C). Interestingly, however, immunoblot analysis detected a high molecular weight Keap1 immunoreactive band in the STHdh^{Q111} cells treated with 3-NP alone, which was not evident when the cells were also treated with DMP (Figure 4A, arrowhead). In 3-NP-treated STHdh^{Q111} cells, protein levels of p62 and Prx-1 increased modestly following pre-treatment with DMP by 40% and 30% on average, respectively (Figures 4D, E); however, due to the great variability of protein expression levels in these cell lines across experiments, these figures were not significant.

Figure 4

A)

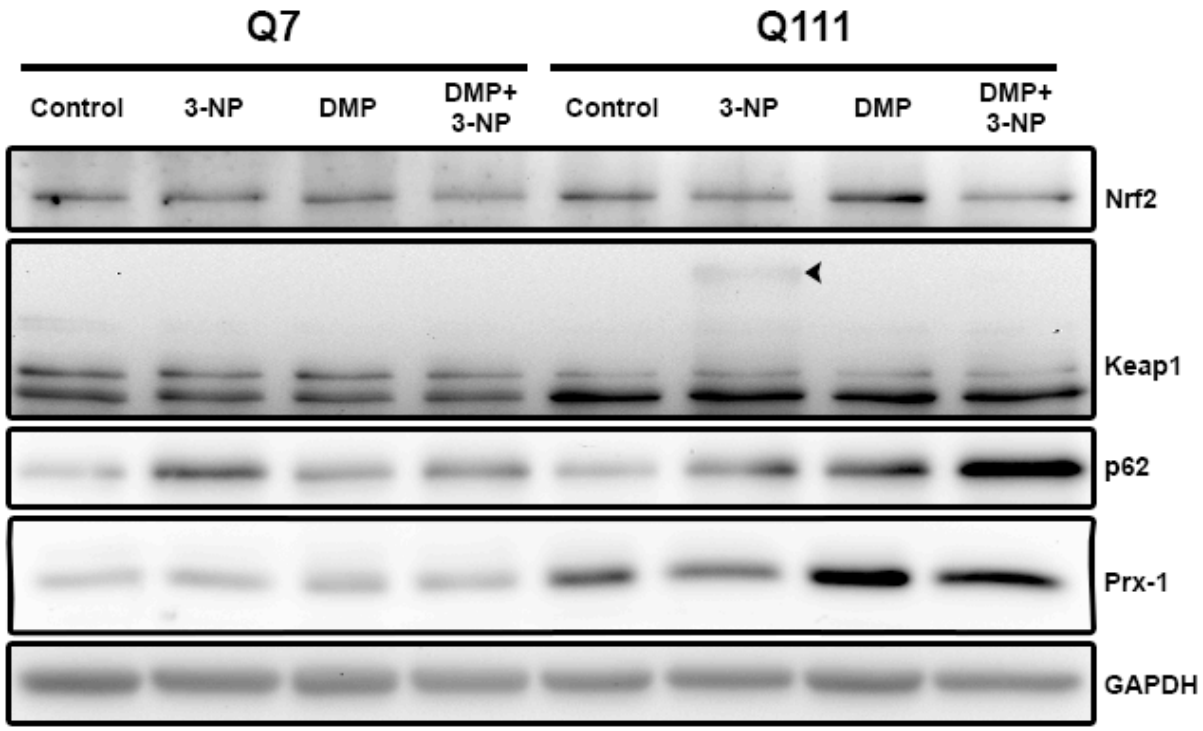
Q7
Q111
Control
3-NP
DMP
DMP+ 3-NP
Control
3-NP
DMP
DMP+ 3-NP
Nrf2
Keap1
p62
Prx-1
GAPDH

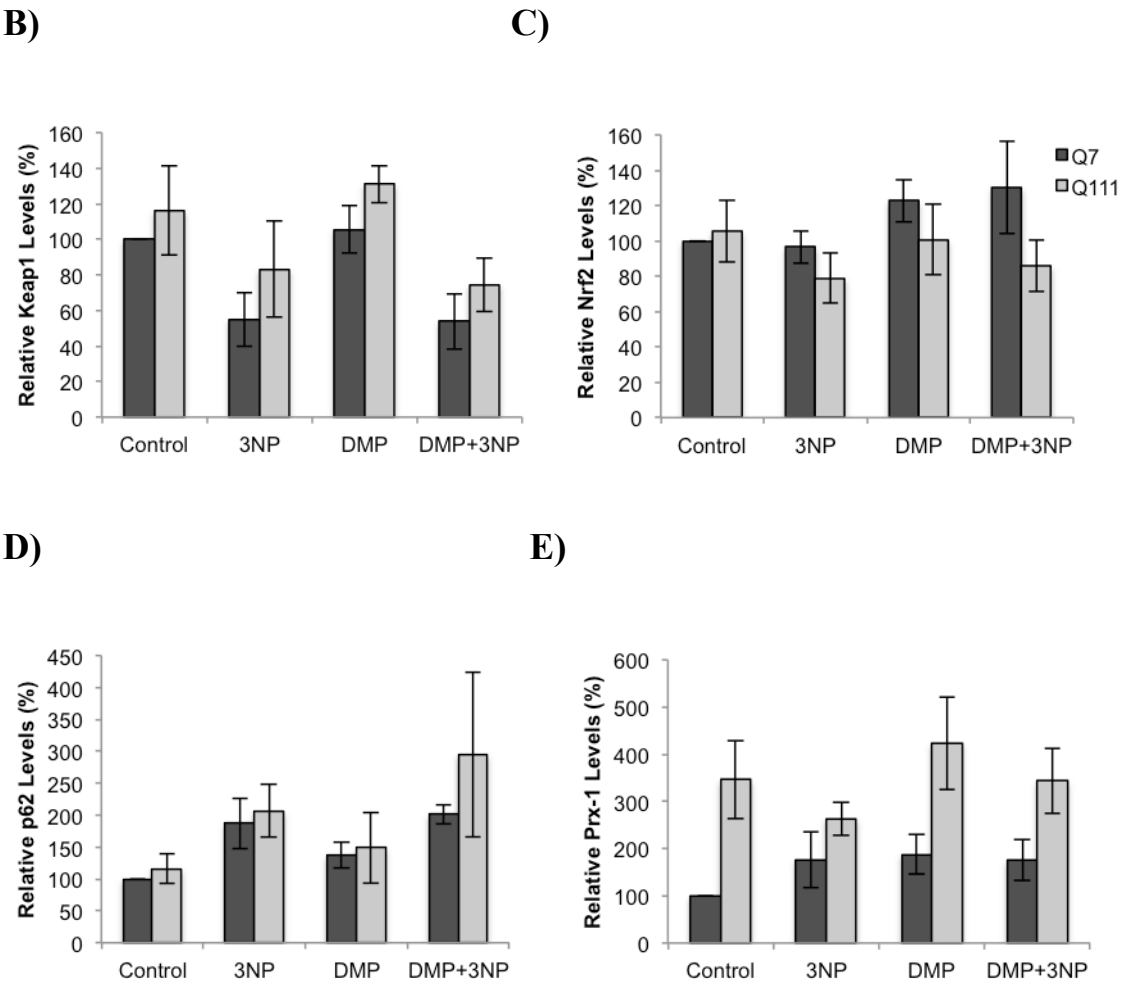

Figure 4. Western blot analysis of protein expression levels in STHdh^{Q7} and STHdh^{Q111} cells. **(A)** Immunoblot analysis of STHdh^{Q7} and STHdh^{Q111} whole cell lysates revealed that DMP does not significantly affect overall Nrf2 or Keap1 protein levels. Protein levels of both p62 and Prx-1 appear to be elevated following treatment of STHdh^{Q111} with DMP. Arrowhead denotes high molecular weight Keap1 immunoreactive band present only in 3-NP-treated STHdh^{Q111} cells. **(B – E)** Densitometric analyses revealed no significant impact of DMP on protein levels of any of the proteins examined. Protein levels of GAPDH were used as a loading control. Error bars represent standard error of the mean derived from three independent experiments.

3.4 DMP promotes the nuclear translocation of Nrf2

Although DMP does not appear to impact overall protein levels of Keap1 or Nrf2, studies have shown that a number of Nrf2 activators merely facilitate the nuclear translocation of Nrf2, thereby increasing its activity (Jain et al., 2005). Thus, the next step was to perform a nuclear fractionation followed by immunoblot analysis to determine if DMP acts by promoting the nuclear translocation of Nrf2. Subcellular fractionation of $STHdh^{Q7}$ and $STHdh^{Q111}$ cells was performed to isolate cytosolic and nuclear protein extracts, which were then screened by immunoblotting using primary antibodies for Nrf2, Keap1, and p62. As expected, $STHdh^{Q7}$ cells exhibited a moderate decrease in cytosolic Nrf2 and a corresponding increase of nuclear Nrf2 following treatment with 3-NP; however this was not observed in the $STHdh^{Q111}$ cell lines, which actually exhibited a substantial decrease in cytosolic Nrf2 with no change in nuclear Nrf2 levels (Figures 5A and 5B). Following treatment with DMP, however, $STHdh^{Q111}$ cells did exhibit higher nuclear Nrf2 levels, and this persisted even when cells were then treated with 3-NP (Figures 5A and 5B). The subcellular localization of neither Keap1 nor p62 appeared to be affected by treatment with DMP (Figures 5A and 5B). Densitometric analysis revealed a trend showing that nuclear Nrf2 levels were indeed increased following DMP treatment in $STHdh^{Q111}$ cells, although these numbers are not significant. A number of time-consuming modifications had to be made to optimize the antibody and fractionation protocol in order to detect the low levels of Nrf2, which is why the values shown for Nrf2 are derived from one experiment (Figure 5C). Analysis of Keap1 and p62 levels revealed no significant change in subcellular localization in neither $STHdh^{Q7}$ nor $STHdh^{Q111}$ cells (Figures 5D, 5E). Due to the high variability in protein expression levels in these cell lines, even under control conditions, a larger number of replicates will be required to solidify these findings.

Figure 5

A)

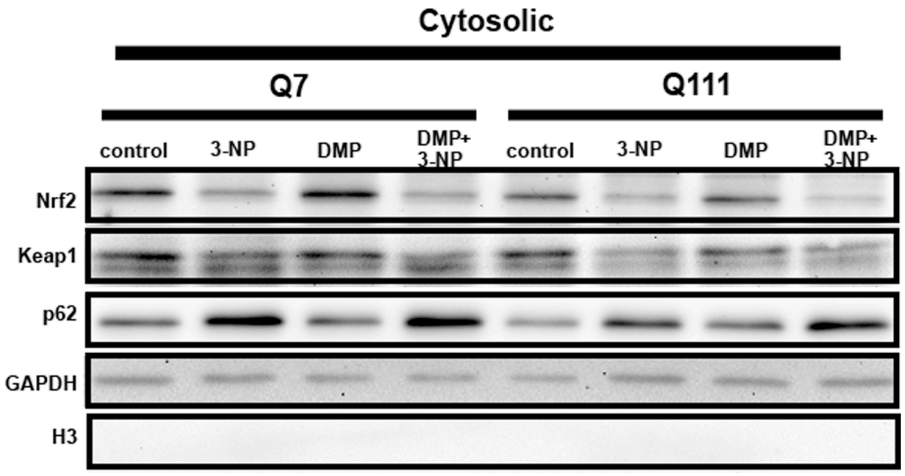
Cytosolic
Q7
Q111
control
3-NP
DMP
DMP+ 3-NP
control
3-NP
DMP
DMP+ 3-NP
Nrf2
Keap1
p62
GAPDH
H3

B)

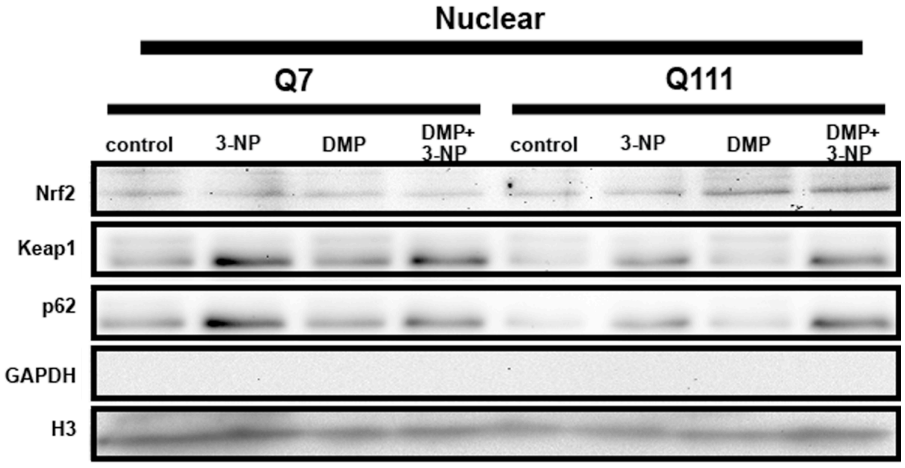
Nuclear
Q7
Q111
control
3-NP
DMP
DMP+ 3-NP
control
3-NP
DMP
DMP+ 3-NP
Nrf2
Keap1
p62
GAPDH
H3

C)

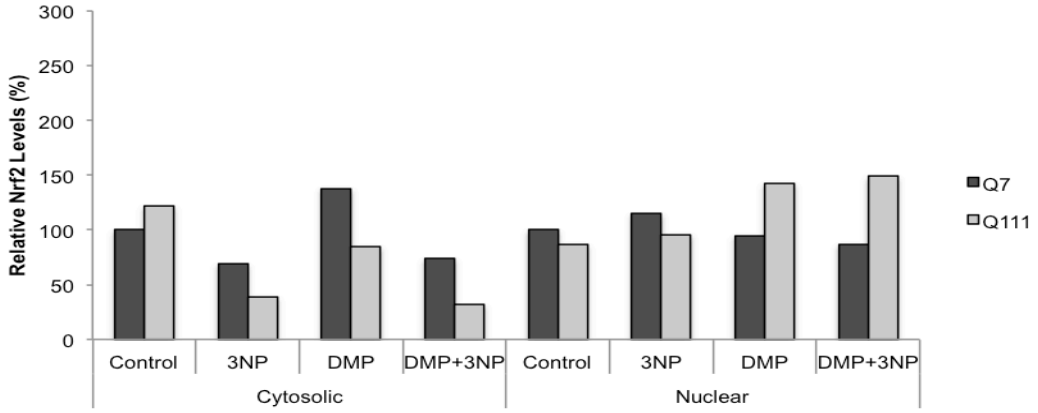
Relative Nrf2 Levels (%)
300
250
200
150
100
50
0
Control
3NP
DMP
DMP+3NP
Control
3NP
DMP
DMP+3NP
Cytosolic
Nuclear
Q7
Q111

D)

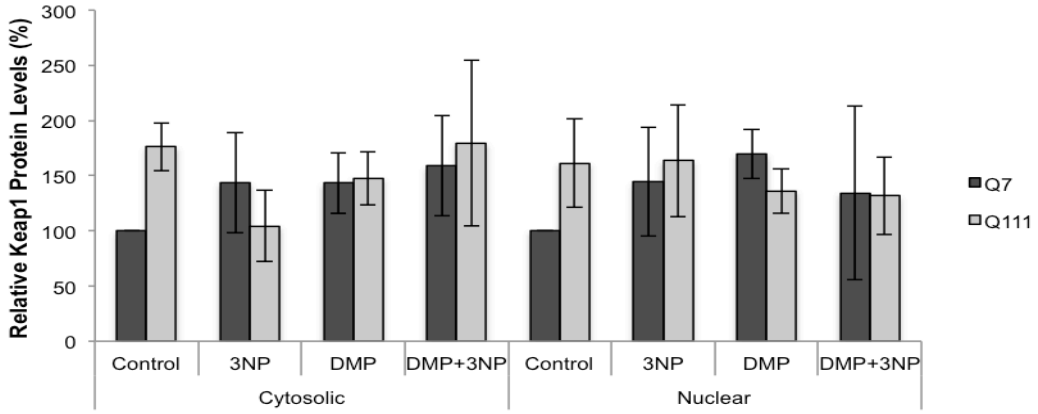
Relative Keap1 Protein Levels (%)
300
250
200
150
100
50
0
Control
3NP
DMP
DMP+3NP
Control
3NP
DMP
DMP+3NP
Cytosolic
Nuclear
Q7
Q111

E)

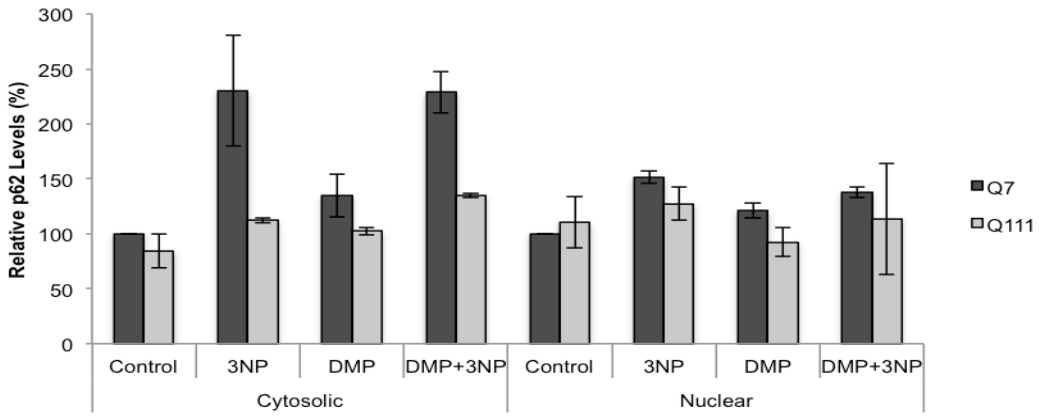

Figure 5. Western blot analysis of cytosolic and nuclear proteins in STHdh^{Q7} and STHdh^{Q111} cells. Immunoblot analysis of **(A)** cytosolic and **(B)** nuclear proteins in both STHdh^{Q7} and STHdh^{Q111} cells following 24 hours of treatment with 10mM 3-NP, with or without 10μM DMP pre-treatment revealed an increase in nuclear Nrf2 levels of STHdh^{Q111} cells following DMP treatment. (C) Densitometric analysis of Nrf2 showing an insignificant trend toward increasing nuclear Nrf2 levels following DMP treatment. Due to technical difficulties and time constraints, values for Nrf2 protein levels are derived from only one experiment. (D and E) Densitometric analyses of Keap1 and p62 protein levels, respectively, reveal substantial variability across treatment groups, with no significant changes following DMP treatment. Error bars represent standard error of the mean derived from three independent experiments.

3.5 DMP promotes the nuclear localization of exogenous Nrf2, while reducing the number of Keap1-positive puncta

Since Nrf2 is maintained at such low levels in these cells, an over-expression construct was used for easier detection. STHdh^{Q7} and STHdh^{Q111} cells were transfected with Nrf2-Flag and underwent 24 hours of treatment with vehicle, 10mM 3-NP, 10μM DMP, or both 3-NP and DMP. The cells were then fixed for immunofluorescence staining with anti-Keap1 and anti-Flag antibodies and visualized by widefield fluorescence microscopy. Images were taken at 400x magnification (Figure 6). Nrf2 was found primarily in the nucleus across all treatment groups in the STHdh^{Q7} control cell line (Figure 6A). However, in the STHdh^{Q111} mutant cell line (Figure 6B), Nrf2 was found in both the nucleus as well as diffusely throughout the cytoplasm under basal conditions as well as following treatment with 3-NP. After treatment with DMP, however, Nrf2 appeared to be more concentrated in the nucleus. In addition, Keap1-positive inclusion bodies were detected in the cytosol (arrows) and nucleus (arrow head), under basal and stress-only conditions in the mutant line, but not in the control line (Figure 6B). Unfortunately, due to challenges associated with poor transfection efficiency and post-transfection hypersensitivity, these findings were unable to be replicated.

Figure 6

A)

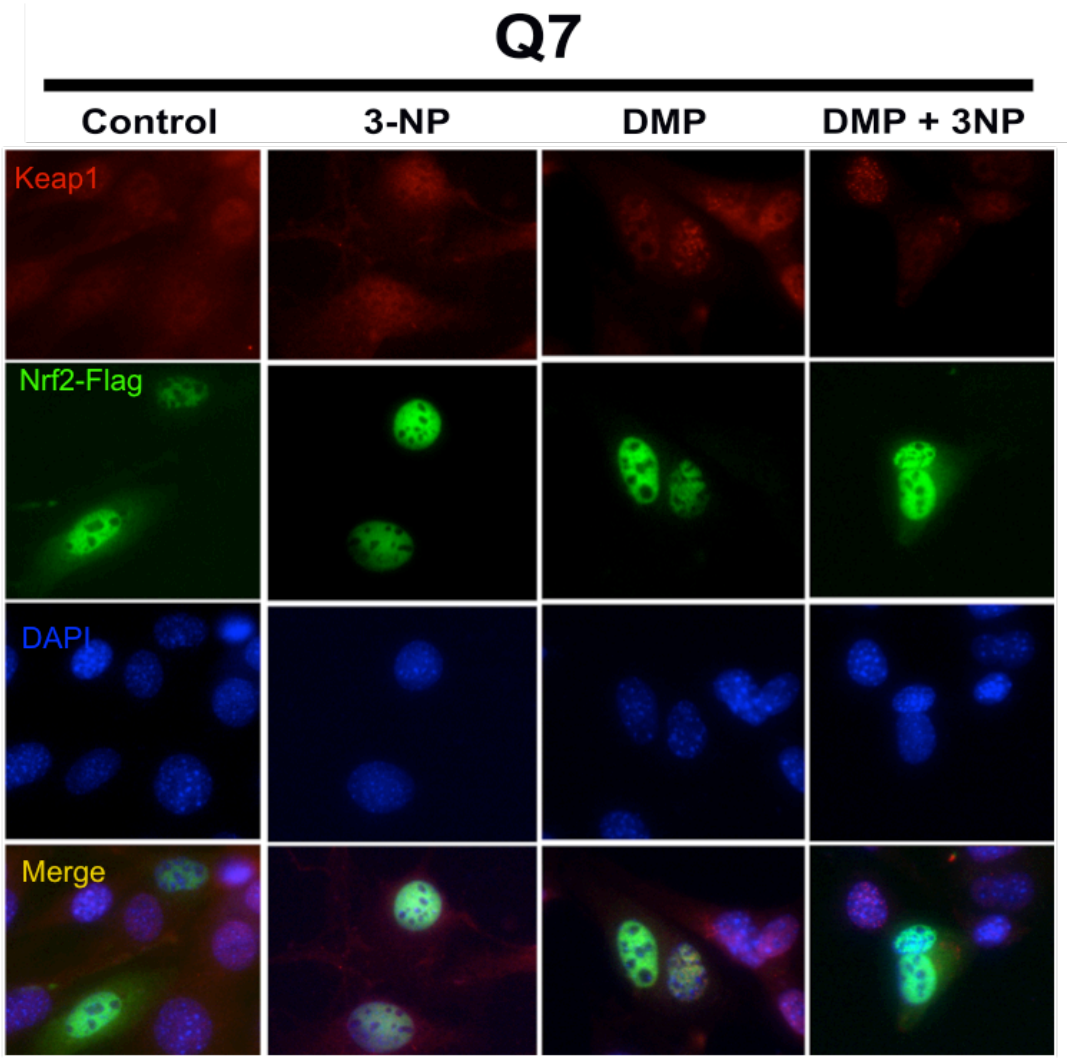

B)

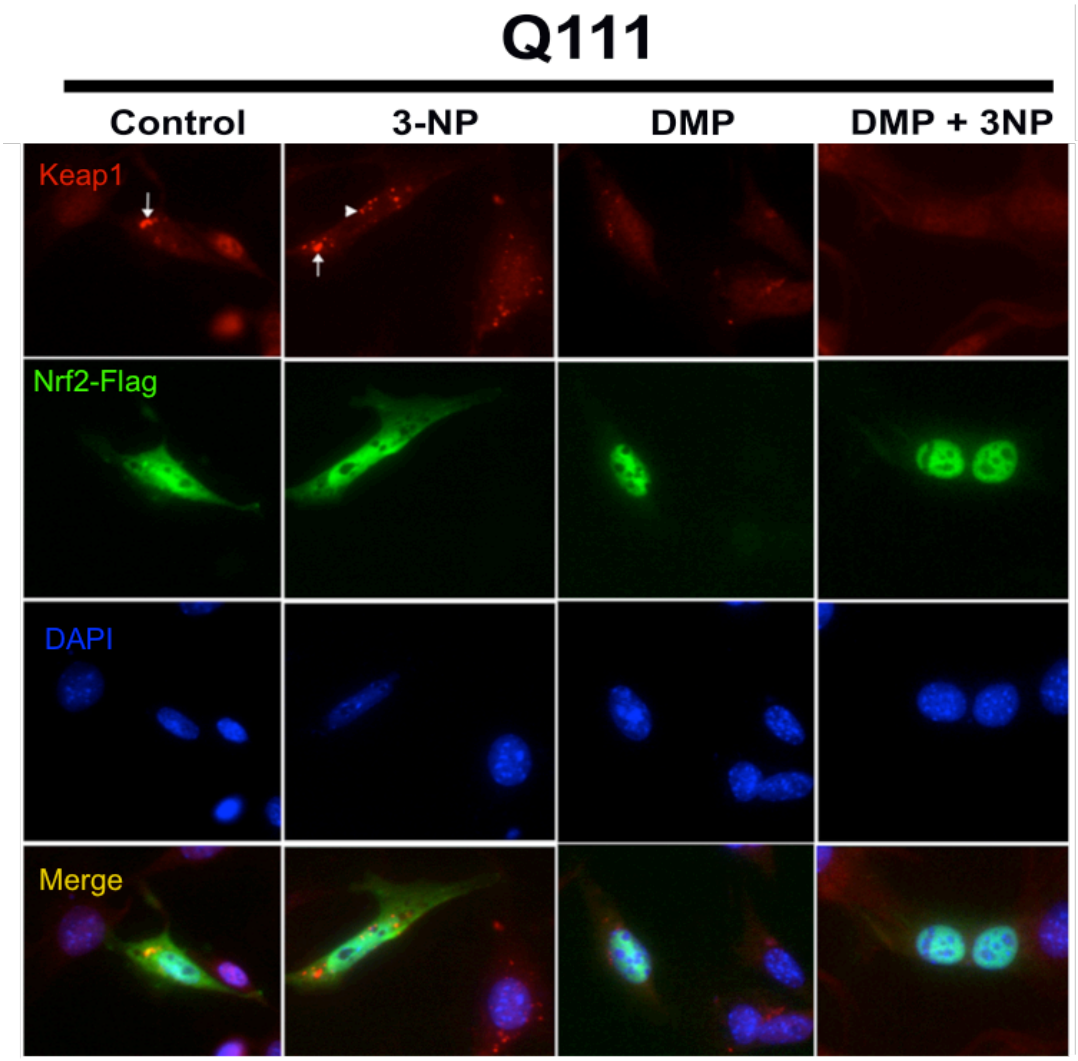

Figure 6. DMP exposure promotes increased Nrf2 nuclear localization and prevents formation of cytoplasmic and nuclear inclusions containing Keap1 in STHdh^{Q111} cells. (A) STHdh^{Q7} and **(B)** STHdh^{Q111} cells were transfected with an Nrf2-Flag expression construct followed by immunofluorescence staining with anti-Flag and anti-Keap1 antibodies. Ectopically expressed Nrf2 was found primarily in the nucleus of STHdh^{Q7} cells under all treatment conditions. In contrast, ectopically expressed Nrf2 was found in both the cytoplasm and nucleus of SThdh^{Q111} cell under both basal conditions and following treatment with 10mM 3-NP. Treatment with 10μM DMP promoted increased Nrf2 nuclear localization. DMP exposure reduced the formation of Keap1-positive cytoplasmic (arrows) and nuclear (arrow head) inclusion bodies in STHdh^{Q111} cells.

3.6 DMP promotes the up-regulation and nuclear translocation of endogenous Nrf2

To further verify that DMP increases nuclear localization of Nrf2, and to accurately compare protein expression levels between treatment groups and cell lines, STHdh^{Q7} and STHdh^{Q111} cells underwent an identical treatment protocol followed by immunofluorescence staining to detect endogenous Nrf2 and Keap1 proteins. Cells were visualized by confocal fluorescence microscopy to allow for more accurate Nrf2 detection even at low expression levels, and images were taken using an immersion oil objective at 400x magnification. STHdh^{Q111} cells exhibit a drastic decrease in both Nrf2 and Keap1 fluorescence intensities following treatment with 3-NP, which is rescued with DMP pre-treatment (Figure 7A). Quantification of fluorescence intensity in 3-NP-treated STHdh^{Q111} cells revealed a two-fold increase in Nrf2 fluorescence following DMP treatment, as well as an increase of Keap1 fluorescence intensity of 50% on average; however, due to the variability across experiments, these values were not significant ($p > 0.05$; Figure 7B).

Figure 7

A)

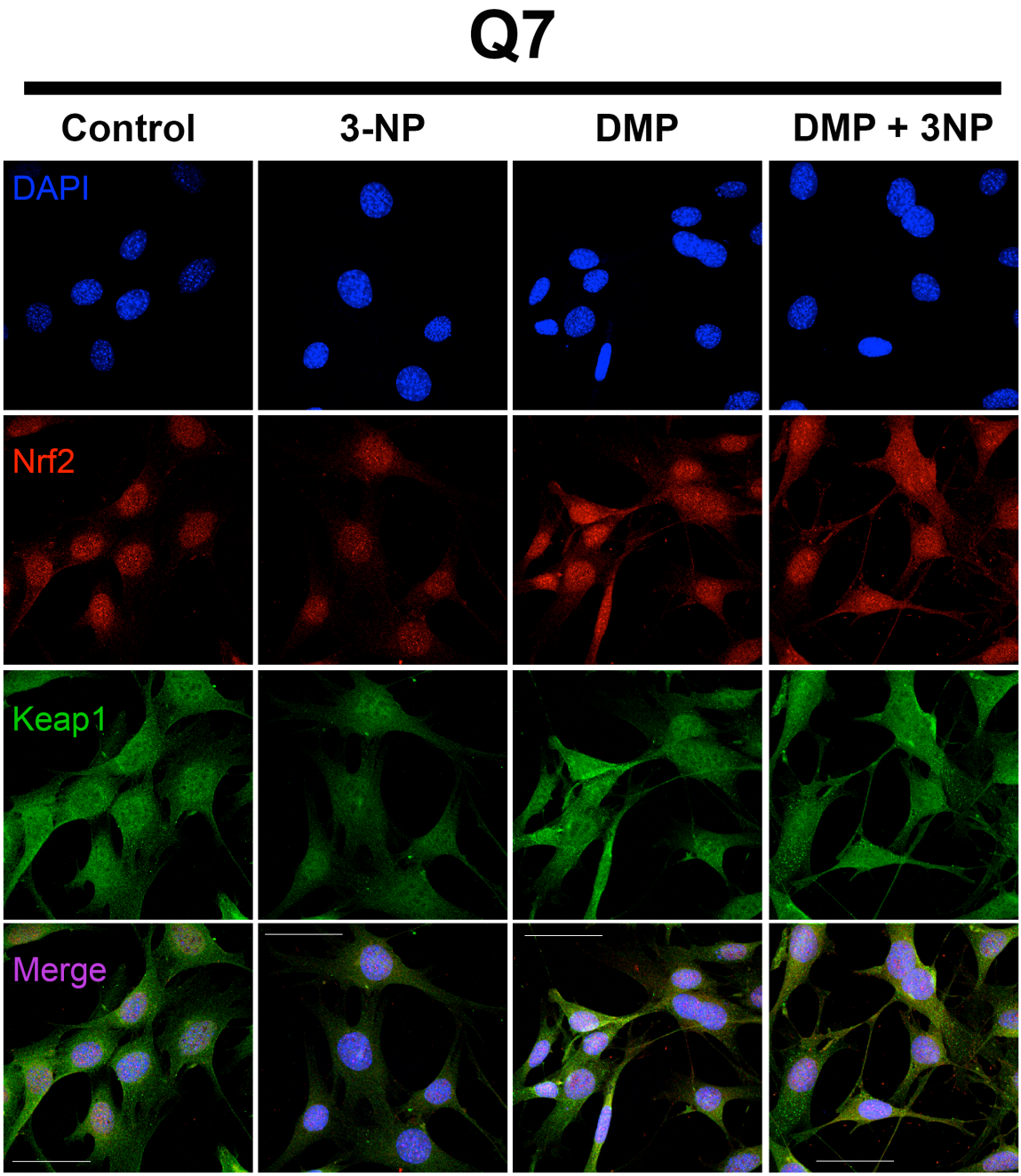

B)

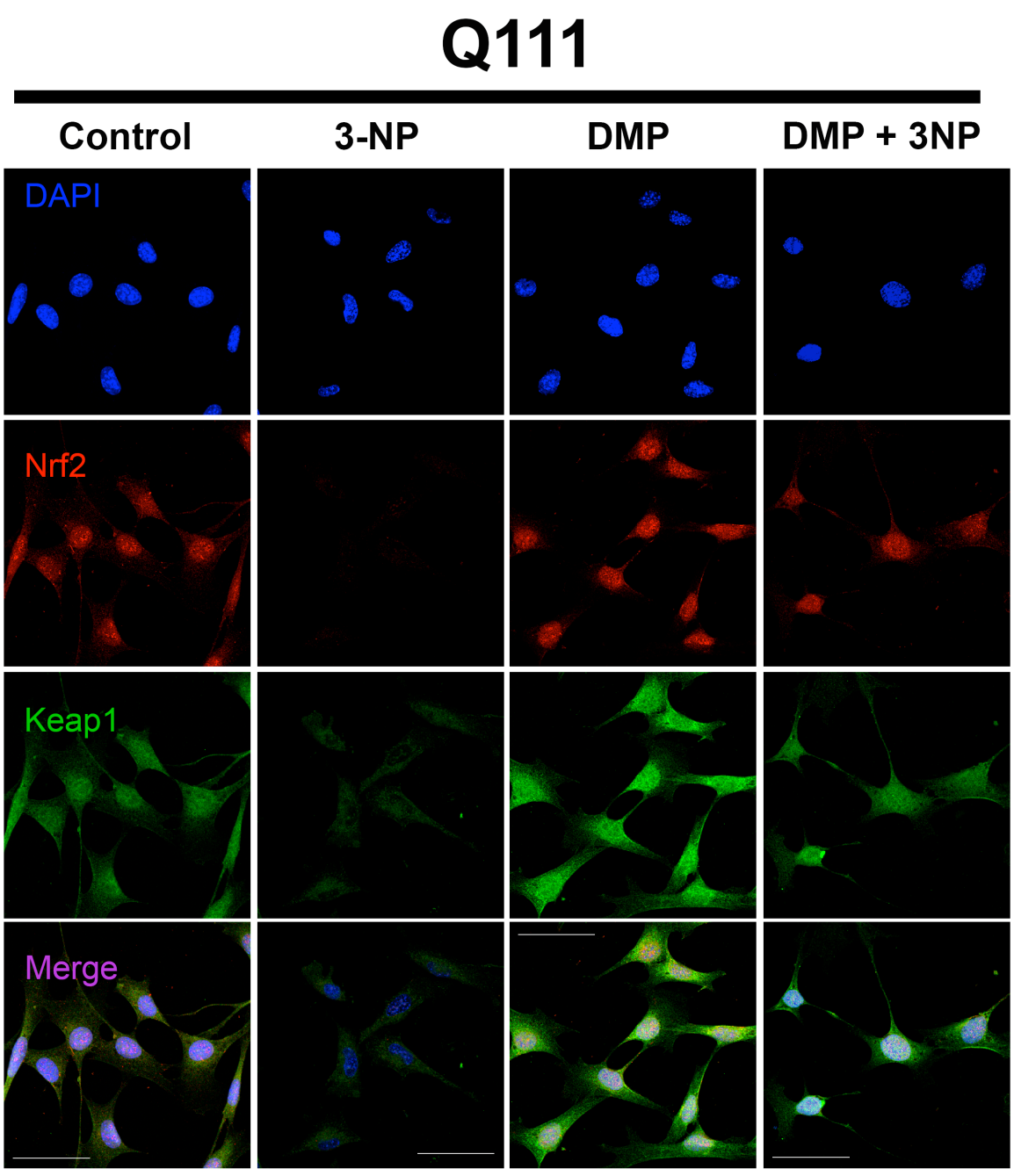

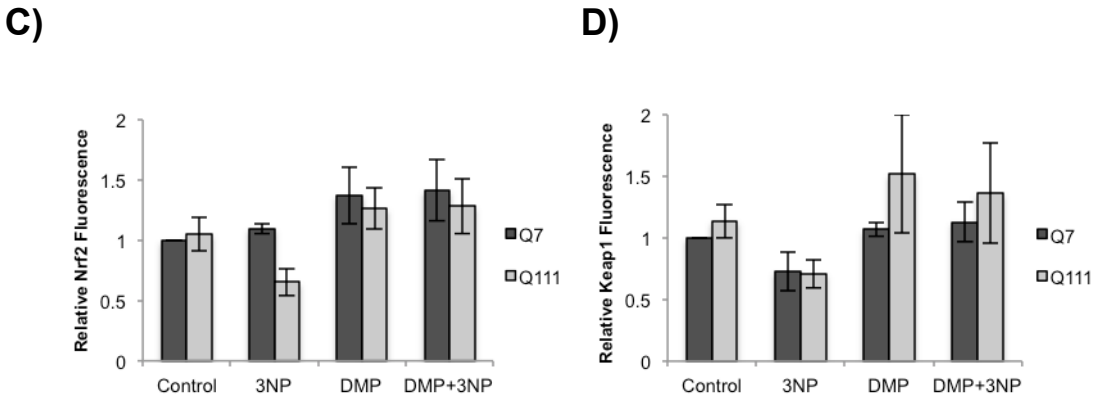

Figure 7. DMP promotes the upregulation and nuclear localization of Nrf2. (A) STHdh^{Q7} and **(B)** STHdh^{Q111} cells were treated with 10mM 3-NP, 10μM DMP, or both for 24 hours, at which point they were fixed and immunostained with anti-Keap1 and anti-Nrf2 antibodies, with nuclei counterstained by DAPI, and imaged via confocal microscopy (Scale bar = 50μm). **(C, D)** Quantification of fluorescence levels for endogenous Nrf2 (left) and Keap1 (right) relative to STHdh^{Q7} control revealed a trend towards an increase in both Nrf2 and Keap1 fluorescence following treatment with DMP, both with and without 3-NP treatment. Error bars represent the standard error of the mean derived from five independent experiments.

3.7 DMP treatment prevents the 3-NP-induced formation of cytoplasmic puncta containing Nrf2 and Keap1 in STHdh^{Q111} cells

To visualize the interaction of Nrf2 and Keap1 in real time, STHdh^{Q111} cells were co-transfected with Nrf2-GFP and Keap1-RFP expression plasmids and treated with 10mM 3-NP, or both 10mM 3-NP and 10μM DMP. They were then placed in a stage-top incubator and visualized by time-lapse widefield fluorescence microscopy. Images were captured at 400x magnification every 15 minutes for 24 hours (Figure 8). Expression of Keap1-RFP resulted in the formation of cytoplasmic inclusion bodies that, in some cells, co-localized with Nrf2-GFP (Figure 8, arrows). The formation of cytoplasmic aggregates containing both Keap1-RFP and Nrf2-GFP was prevented by DMP exposure. Due to the heightened sensitivity to toxins experienced by STHdh^{Q111} cells following transfection, no cells remained alive after 3 hours in the 3-NP-treated group. Unfortunately, due to challenges associated with poor transfection efficiency and post-transfection hypersensitivity, these findings were unable to be replicated.

Figure 8

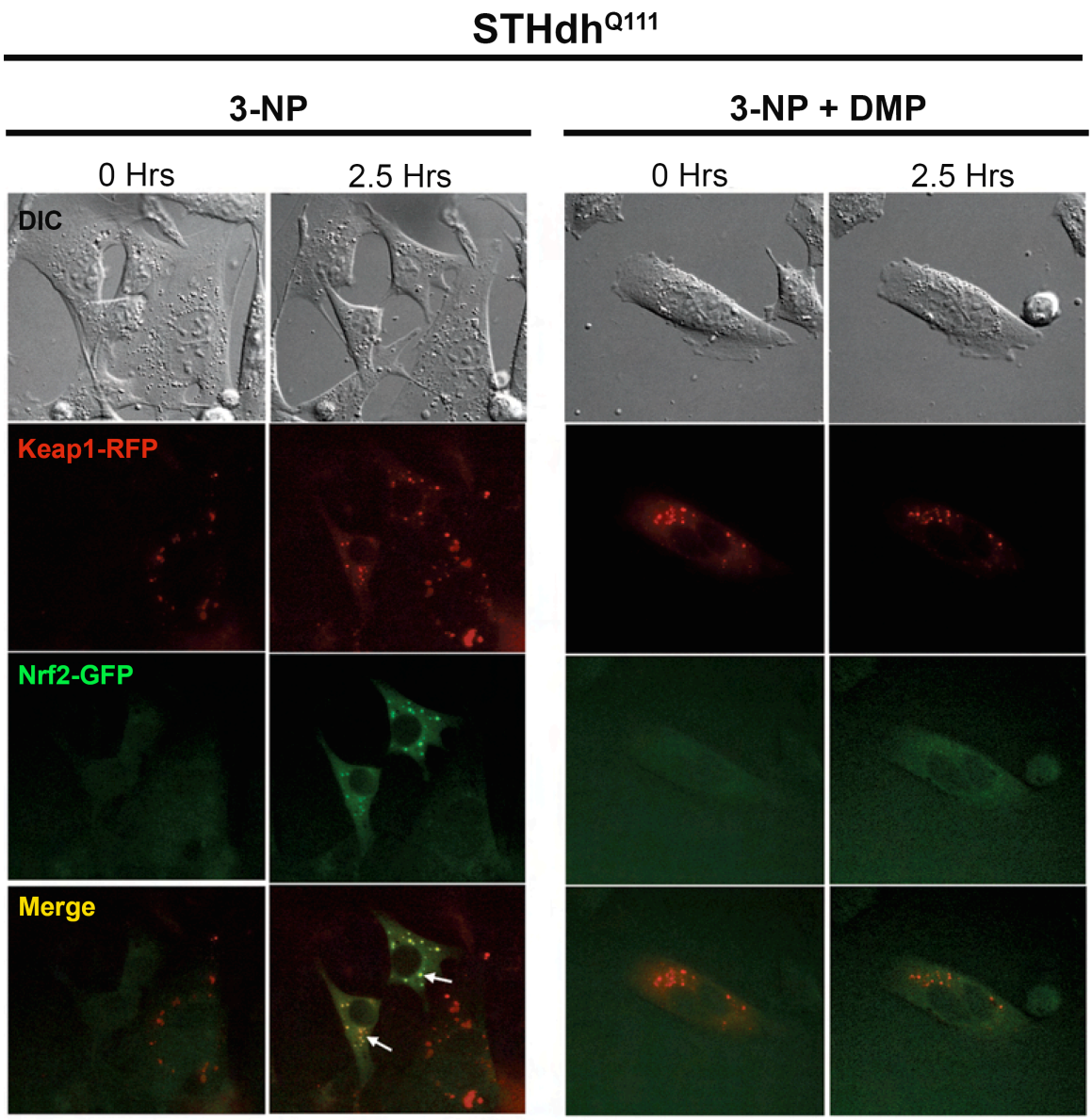

Figure 8. Timelapse fluorescence microscopy reveals formation of cytoplasmic puncta containing both Keap1-RFP and Nrf2-GFP in 3-NP-exposed STHdh^{Q111} cells. STHdh^{Q111} cells were co-transfected with plasmids encoding Keap1-RFP and Nrf2-GFP and then treated with 10mM 3-NP (left two panels) or with both 10mM 3-NP and 10μM DMP (right two panels) and then imaged by widefield fluorescence microscopy (400x magnification). The formation of cytoplasmic puncta containing both Keap1-RFP and Nrf2-GFP (arrows) was prevented by DMP treatment.

3.8 Cytotoxic over-expression of Keap1-RFP can be rescued with DMP treatment in HT22 cells

Due to the poor transfection efficiency and post-transfection survival of STHdh^{Q111} cells, the Keap1-RFP vector was transfected into a more resilient hippocampal cell line (HT22 cells). Cells were then placed in a stage-top incubator, treated with 100μM DMP and visualized by time-lapse widefield fluorescence microscopy. Images were taken every 15 minutes at 400x magnification (Figure 9). The time-lapse images at 0.5 hours (Figure 9 A) and 4.25 hours (Figure 9 B) of ectopically expressed Keap1-RFP in HT22 cells revealed the progressive accumulation of Keap1-RFP in puncta that formed shortly before cell death. In contrast, DMP treatment directed Keap1-RFP to small vesicle-like structures; an event associated with decreased levels of Keap1 and increased cell survival. Unfortunately, there was not enough time to complete replicates of this experiment, and these findings are derived from a single experiment.

Figure 9

A)

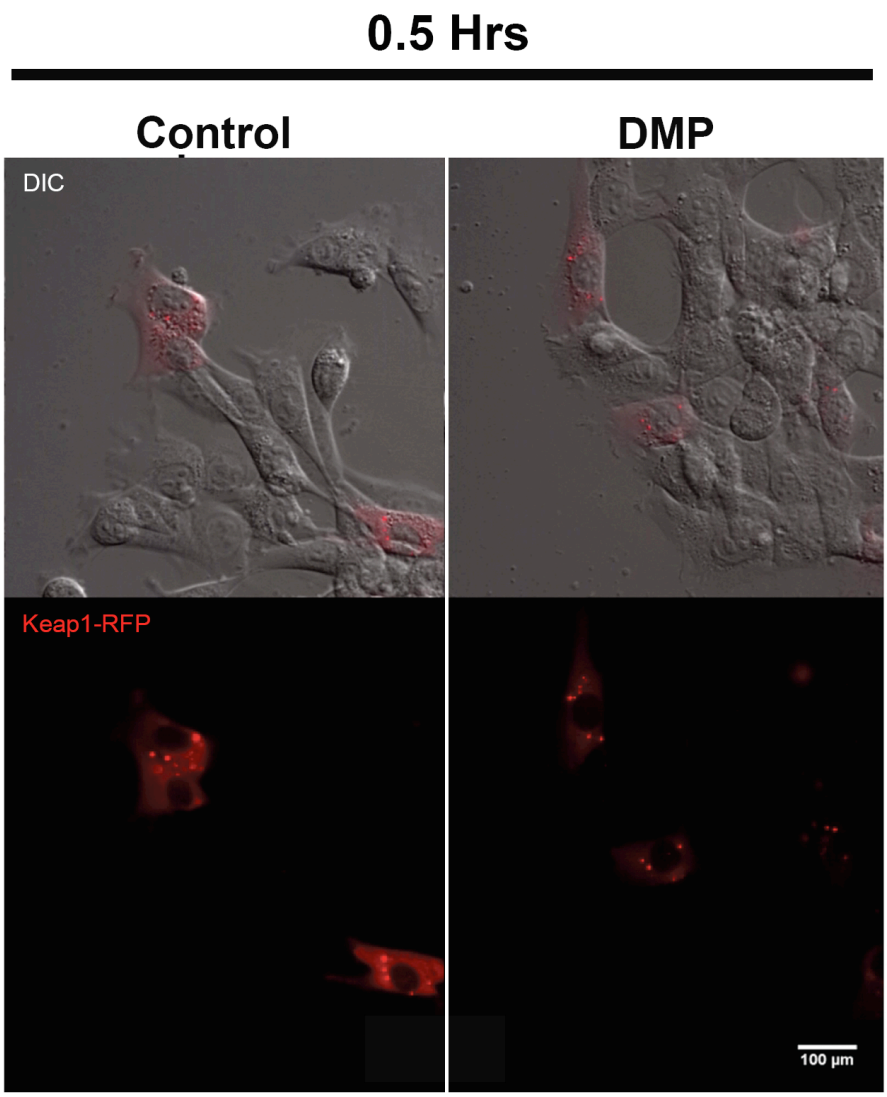

B)

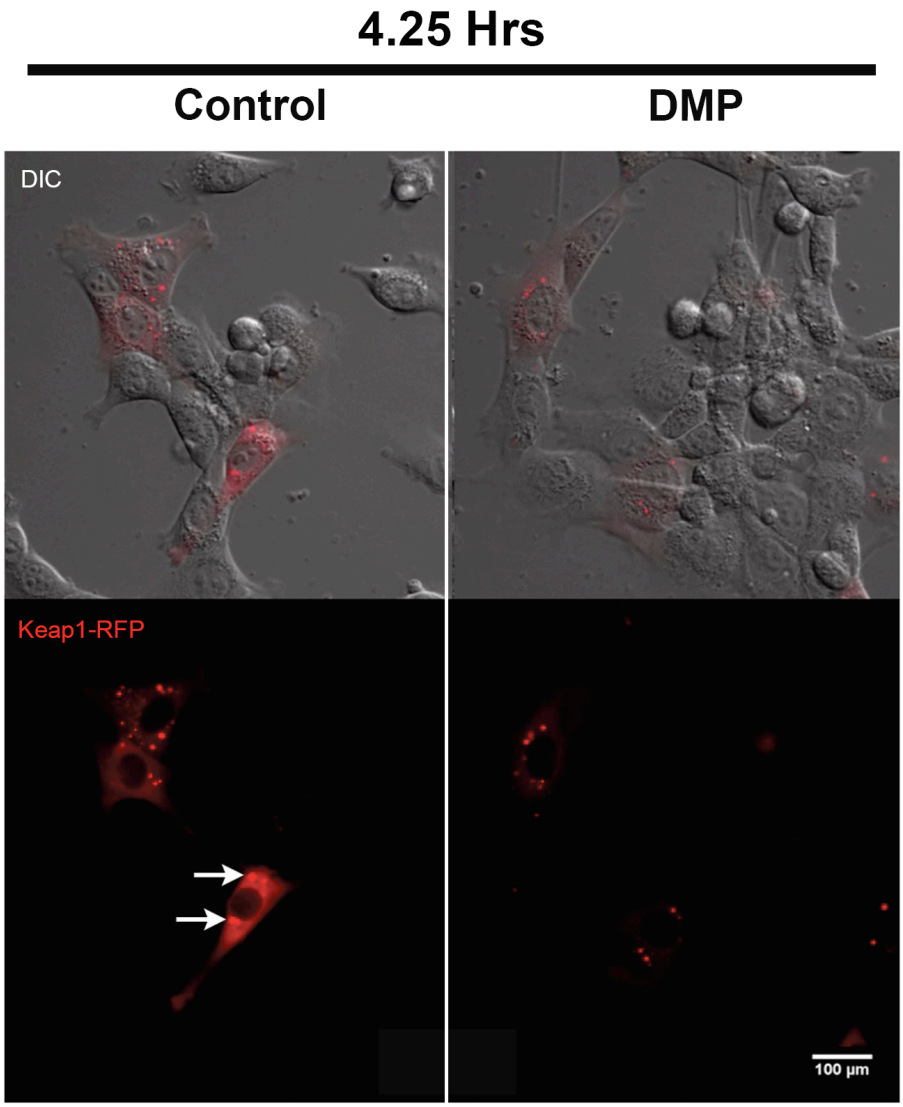

Figure 9. Overexpression of Keap1-RFP leads to the formation of puncta. Time-lapse fluorescence imaging at 0 hours **(A)** and 4.25 hours **(B)** of ectopically expressed Keap1-RFP in HT22 cells revealed the progressive accumulation of Keap1-RFP in puncta (arrows), whose formation strongly correlated with subsequent cell death. Treatment of cells with DMP (100µM) directed Keap1-RFP to small vesicle-like structures and overall decreased fluorescence. Top panels show overlay of DIC and fluorescent micrographs.

Chapter 4 : Discussion

4.1 Overview

Previous studies have provided compelling evidence for the role for antioxidants in treating the oxidative stress-induced pathogenesis of many neurodegenerative disorders, including Huntington's disease (HD; Browne and Beal, 2006). Furthermore, although canonical activators of Nrf2 have been examined extensively, this investigation sought to characterize the mechanisms and neuroprotective potential of a non-canonical Nrf2 activator. The findings of this study suggest that DMP plays a role in reducing oxidative stress thereby mediating resistance to 3-NP and mHTT-induced neurotoxicity in a striatal cell model of HD. Additionally, the neuroprotective nature of DMP did appear to be mediated in part by increased Nrf2 nuclear translocation and activation. Furthermore, DMP does not seem to be activating Nrf2 through the hypothesized non-canonical autophagy pathway, but perhaps through a more novel mechanism.

4.2 DMP confers neuroprotection against 3-NP by reducing mitochondrial ROS levels and oxidative damage-induced neurotoxicity

3-NP is an irreversible complex II inhibitor in the mitochondrial ETC, and when it is administered to rodents in their drinking water, it causes targeted lesions in the striatum, producing symptoms reminiscent of HD (Borlongan et al., 1997). It has also been shown that mitochondrial complex II inhibitors generate ROS by disrupting the ETC (Pérez-Severiano et al., 2004). $STHdh^{Q111}$ cells have a heightened sensitivity to 3-NP compared to the wild-type $STHdh^{Q7}$ cells, owing potentially to their compromised antioxidant defense systems. Cell viability of both striatal cell lines was assessed following treatment with 10mM 3-NP for 24 and 48 hours with or without pre-treatment with 10μM DMP. The findings from both MTT (Figure 2B) and Trypan Blue Exclusion (Figure 2C) assays in this study did not yield significant results in line with previous reports (Pitts et al.,

2012). However, further analysis of cell viability by a more sensitive technique, the LIVE/DEAD Cell Viability/Cytotoxicity assay (Figure 2A), did reveal a significant increase in cell survival in DMP-pre-treated striatal cells (Figure 2A). It is likely that, due to the changes in cell behavior that occur at different striatal cell passage numbers, the variability in toxin sensitivity is high enough that crude tests such as the trypan blue exclusion assay are unable to accurately report the relative number of viable cells. Furthermore, although cells were rinsed twice in an effort to remove all traces of treatment drug, it is possible that residual 3-NP interfered with the MTT assay, thus confounding the results. In addition, this study found that DMP mediated protection against mHTT- and 3-NP-induced neurotoxicity correlated with a decrease in mitochondrial ROS levels. Following treatment with 10mM 3-NP, STHdh^{Q111} cells exhibited a significant increase in MTR fluorescence intensity, which was ameliorated in DMP-pre-treated cells (Figure 3). In contrast, STHdh^{Q7} control cells under the same treatment conditions did not show increased mitochondrial ROS following 3-NP treatment. Therefore, these results taken together indicate that DMP may elicit neuroprotection by reducing the levels of mitochondrial ROS and thus the extent of oxidative damage caused by 3-NP.

4.3 DMP increases nuclear Nrf2 protein levels

The Nrf2-Keap1-ARE pathway is a redox-sensitive signaling axis, which regulates the expression of a wide variety of cytoprotective proteins and phase II detoxifying enzymes to protect the cell against oxidative stress, and harmful toxins. Under basal conditions, Nrf2 is maintained at very low levels in the cell due to contant proteosomal degradation. Nrf2 levels fluctuate in rapid response to the changing intracellular environment, which allows it to translocate to the nucleus and increase expression of these protective genes in order to preserve redox homeostasis in mammalian cells. However, previous studies have reported Nrf2 dysregulation in a number of neurodegenerative diseases (Ramsey et al., 2007), and even more have established the link between elevated ROS and neurodegenerative disease (Berlett and Stadtman, 1997; Butterfield and Kanski, 2001; Mariani et al., 2005). In addition, Nrf2 nuclear translocation deficits have been reported

in other trinucleotide repeat neurodegenerative disorders such as Friedrich's ataxia (Paupe et al., 2009). Classical, or canonical, activators of Nrf2 mimic a transient oxidative insult by modifying specific Keap1 cysteine residues, leading to the dissociation and stabilization of Nrf2. This allows Nrf2 protein levels to increase within the cell, which promotes Nrf2 nuclear localization where it dimerizes with small Maf proteins and binds to the cis-acting regulatory element known as the antioxidant response element (ARE; He and Ma, 2010).

A previous graduate student in the Cumming lab provided evidence, via the ARE-luciferase assay, that DMP activates Nrf2 and increases ARE-directed gene expression in an mHTT-inducible PC12 model of HD (Dailey, 2012). Unfortunately, due to challenges associated with poor transfection efficiency using the appropriate vectors, as well as heightened toxin sensitivity post-transfection, this experiment could not be replicated in the striatal cell lines. However, preliminary results from immunoblot analysis of nuclear fractionation experiments, as well as immunofluorescence studies of both exogenous and endogenous Nrf2 suggest that treatment with DMP promotes a modest nuclear accumulation of Nrf2, which persists in the presence of the mitochondrial stressor, 3-NP (Figures 5, 6, 7). Regrettably, the values presented for the immunoblot analysis of Nrf2 levels in subcellular fractions are derived from only one experiment. This is partially attributable to the number of changes that had to be made to optimize the fractionation protocol. Additionally, due to the extremely low levels of basal Nrf2 in the striatal cell lines, the ongoing controversy as to the correct molecular weight and which antibodies to use, as well as the high sensitivity of STHdh^{Q111} cells to 3-NP, it was a challenge to detect Nrf2 following cell fractionation (Lau et al., 2013). Therefore, additional replicates will need to be conducted using the appropriate protocols and antibodies in order to solidify these findings. In order to solidify the claim that DMP activates Nrf2 in these striatal cell lines, further studies should be completed in which transcriptional activity of Nrf2 is more accurately assessed: either through modifications to the ARE-luciferase assay, by using an Nrf2 Transcription Factor Assay Kit (Cayman Chemicals), or, alternatively, via quantitative real-time polymerase chain reaction of downstream Nrf2 target proteins (such as Prx-1), performed both with and without DMP treatment.

More recently, evidence has accumulated supporting an alternative model of Nrf2-Keap1 signaling: in this proposed model, newly translated Nrf2 translocates into the nucleus and binds the ARE to maintain basal expression cytoprotective proteins. Afterwards, Nrf2 dissociates from the ARE and binds with nuclear Keap1, which facilitates the poly-ubiquitylation and subsequent nucleocytoplasmic shuttling of Nrf2 to the cytosol for degradation via the 26 S proteasome (Nguyen et al., 2005). Cell culture studies have revealed that the nucleocytoplasmic properties of Keap1 act via the Chromosomal Maintenance (CRM1)/Exportin1 pathway, and the inhibition of this pathway leads to an accumulation of nuclear Keap1 and a decrease in Nrf2 activity (Karapetian et al., 2005). Experiments using an over-expression Keap1 vector and the CRM1/Exportin inhibitor, Leptomycin B (LMB), showed that canonical Nrf2 activator *tert*-butylhydroquinone (tBHQ) did not interfere with Keap1's ability to enter the nucleus, which is thought to involve the nuclear import protein, p65 (Nguyen et al., 2005; Yu et al., 2011). Interestingly, the researchers that reported these findings also revealed that the fluctuations in Keap1 and Nrf2 protein levels were so minute that they could not be detected without using overexpression constructs as well as import inhibitors and proteasomal inhibitors, respectively (Nguyen et al., 2005). Future studies should investigate whether DMP activates Nrf2 through this novel pathway, perhaps by interfering with the translocation of Keap1 into the nucleus, or by inhibiting the binding of nuclear Keap1 to Nrf2 (Figure 10). This could be observed by using Keap1 overexpression constructs in a more transfection-tolerant cell line and by performing nuclear fractionation followed by immunoblot analysis of nuclear Keap1 levels with and without DMP treatment.

Figure 10

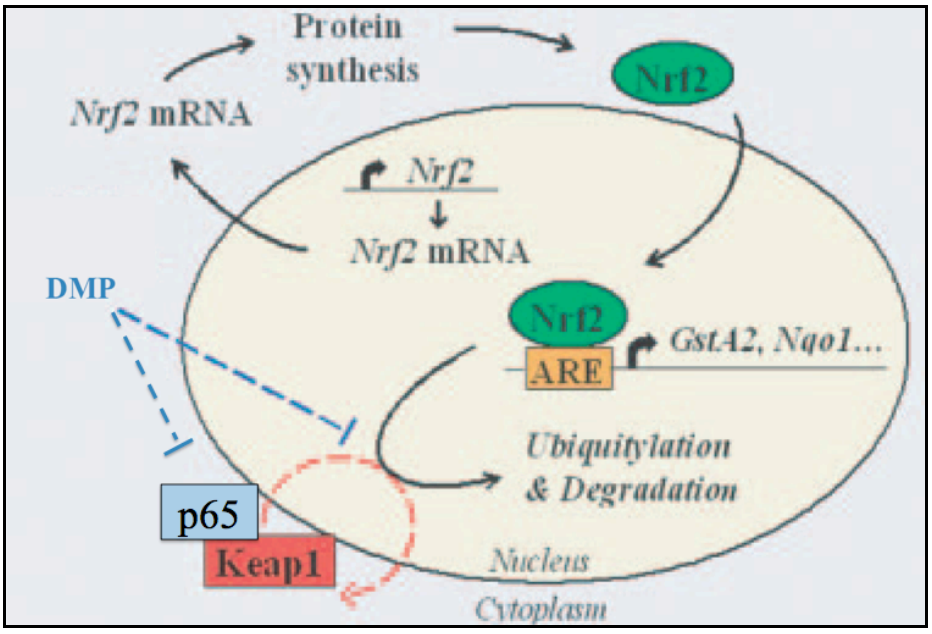

Figure 10. Schematic illustration of a proposed alternative model of the Nrf2-Keap1 pathway of gene regulation (modified from Nguyen et al., 2005). In this model, newly translated Nrf2 translocates into the nucleus and binds the ARE to maintain basal expression cytoprotective proteins. Afterwards, Nrf2 dissociates from the ARE and binds with nuclear Keap1, which facilitates the poly-ubiquitylation and subsequent nucleocytoplasmic shuttling of Nrf2 to the cytosol for degradation via the 26 S proteasome. It is possible that DMP activates Nrf2 through this pathway, either by inhibiting the binding of Nrf2 to Keap1 within the nucleus, or by impairing the ability of Keap1 to enter the nucleus at all.

4.4 DMP activates Nrf2 via a non-canonical mechanism

Earlier studies, as well as data presented here, have shown that DMP is protective against mHTT-induced toxicity in the same PC12 cell line, and 3-NP-induced toxicity in STHdh^{Q111} cells (Pitts et al., 2012). However, when the protection against 3-NP-induced toxicity elicited by DMP was compared to that of a canonical Nrf2 activator, sulforaphane, it became evident that its protective effects are not due to Nrf2 activation alone: while DMP enhanced viability in 3-NP-treated STHdh^{Q111} cells with an optimal concentration of 10μM, sulforaphane was not protective and actually potentiated 3-NP-induced toxicity at concentrations above 0.5μM (Appendix: Figure I). These observations suggest that, although both compounds are capable of Nrf2 activation, DMP may utilize a non-canonical mechanism of Nrf2 activation that is particularly protective against 3-NP toxicity. Recently, studies have elucidated a non-canonical, p62-dependent induction of Nrf2. This mechanism involves the direct interaction between p62 and Keap1 such that Keap1 is sequestered into autophagosomes for degradation, which disrupts the ubiquitination of Nrf2, allowing for activation of the Nrf2 pathway (Komatsu et al., 2010; Lau et al., 2010). Interestingly, p62 overexpression significantly decreases the half-life of Keap1, while p62 knockdown increases it; this implies that p62 plays a crucial role in regulating Keap1 turnover (Copple et al., 2010). Comparative analysis of STHdh^{Q7} and STHdh^{Q111} whole cell lysates revealed that overall Keap1 protein levels were not reduced following DMP treatment (Figure 4), which does not support the hypothesis of this study, in which DMP promotes Nrf2 activity through the p62-mediated autophagosomal degradation of Keap1. However, taking into account the trend toward increased p62 levels following DMP treatment, it would be prudent to perform additional experiments

examining overall Keap1 protein levels at a number of time points aside from 24 hours before claiming that DMP is not promoting autophagosomal degradation of Keap1.

4.5 DMP exposure inhibits the formation of cytoplasmic and nuclear inclusion bodies containing Keap1

Ubiquitinated protein inclusions are a hallmark of many neurological disorders, including polyglutamine disorders such as HD, and it has been well established that, in HD, the mHTT protein misfolds causing the formation of nuclear and cytosolic inclusion bodies. Interestingly, recent findings revealed that Keap1 co-localizes to neuronal cytoplasmic inclusions in various neurodegenerative disorders (Tanji et al., 2013). Closer examination of immunofluorescence data from striatal cells transfected with Nrf2-Flag, which were co-stained to detect endogenous Keap1, revealed the presence of Keap1-positive cytoplasmic inclusion bodies, some of which co-localized with Nrf2-Flag, in the $STHdh^{Q111}$ but not $STHdh^{Q7}$ cells (Figure 6). Interestingly, these inclusion bodies were only detected under basal and 3-NP treatment conditions, suggesting that DMP treatment decreased the formation of these Keap1 inclusion bodies, both in the presence and absence of 3-NP. Furthermore, visualization of Keap1-RFP and Nrf2-GFP in $STHdh^{Q111}$ cells by time-lapse fluorescence microscopy also revealed the formation of cytoplasmic inclusion bodies containing both exogenous proteins; these inclusion bodies were also prevented by DMP exposure (Figure 8). In addition, closer examination of immunoblot analysis of whole cell lysates revealed a high-molecular weight Keap1 band in 3-NP treated $STHdh^{Q111}$ cells, which could be reflective of an aggregated form of Keap1 (Figure 4). Separate experiments performed in the Cumming lab also found that co-expression of Keap1-RFP with mHTT-GFP in the PC12-103Q cell model of HD resulted in co-localization of both proteins in large puncta, which are prevented by DMP exposure (Appendix: Figure II). Although the role that protein aggregates play in neurotoxicity remains unclear, there is a strong argument that the elimination of these inclusions may be effective in attenuating neurodegenerative pathogenesis. Some studies have provided evidence for an inherent toxicity of aggregation of some proteins not implicated in any diseases, which suggests that perhaps the abnormal protein conformation is, in its self,

cytotoxic (Bucciantini et al., 2002). To further assess the inherent cytotoxic properties of aggregated Keap1, time-lapse fluorescence imaging of ectopically expressed Keap1-RFP was performed in a more transfection-tolerant hippocampal cell line (HT22 cells). This experiment revealed a progressive accumulation of Keap1-RFP inclusion bodies that preceded cell death. In contrast, DMP treatment directed Keap1-RFP to small vesicle-like structures, which was correlated with prolonged cell survival (Figure 9). These findings indicate that DMP may work through an autophagosomal mechanism; however, it may be simply preventing the sequestration of Keap1 and Nrf2 into these puncta. Future studies should focus on immunoprecipitation assays to look for changes in direct interactions between Keap1–Nrf2, Keap1–p62, and Keap1–mHtt following DMP treatment. Additionally, it would be beneficial to observe the interactions and subcellular localization of these key proteins via time-lapse fluorescence microscopy in a cell line that is more tolerant of transfection reagents.

4.6 Analysis of the different cell culture models of HD

A number of *in vitro* models have been developed to study the intracellular mechanisms associated with HD pathology; cell culture models are also often the starting point in identifying the beneficial targets of novel pharmacotherapy agents. An increase in mHTT aggregates has been strongly associated with toxicity in *in vitro* models of HD (Hackam et al., 1998), and expression of the truncated mHTT is representative of a delayed disease progression, whereas expression of the full-length mHTT protein would more accurately depict the natural disease progression (Dong et al., 2012). The commonly used PC12-103Q and PC12-25Q cell lines, which were used in previous studies in this lab, are immortalized cells derived from a rat pheochromocytoma, which have been transfected with an ecdysone-inducible protein containing the first 17 amino acids of HTT plus 103 or 25 glutamines fused with enhanced GFP. Although some aspects of the pathological role of mHTT can be effectively studied in these cells, HD involves the targeted degeneration of striatal MSNs, which are characteristically distinct from PC12 cells. Additionally, PC12 cells express only a truncated version of the mHTT protein, and the protein's fusion to GFP likely increases its predisposition for aggregation and therefore

toxicity. The cell lines used in this investigation are immortalized cells derived from the striatum of transgenic mouse models of HD that have either 7 ($STHdh^{Q7}$) or 111 ($STHdh^{Q111}$) CAG repeats within exon 1 of the mHtt gene, and express the full length wild-type and mutant HTT, respectively (Trettel et al., 2000). Although these cells express the full-length HTT protein, and are more representative of MSNs, there are a number of drawbacks associated with their use. Firstly, the transfection efficiency of the striatal cells was quite poor, and seemed to cause hypersensitivity to xenobiotic and oxidative stress, especially in the $STHdh^{Q111}$ cells. This made the use of overexpression constructs for immunofluorescence and live cell fluorescence experiments difficult and questionable; very few cells retaining both the Nrf2-GFP and Keap1-RFP constructs survived treatment, and, by imaging the few that did, we may have been selecting for a transfection-tolerant cell type. The protein expression levels and oxidative stress sensitivity also seemed to vary substantially depending on the passage number, which made the completion of experimental replicates problematic. Furthermore, as indicated by the Coriell Institute, after passage number 10-12 the mHTT protein is no longer reliably expressed, so cells were not used after passage number 10. In addition, this investigation revealed that the $STHdh^{Q111}$ cells also do not display differential sensitivity to 3-NP treatment compared to $STHdh^{Q7}$ when they are both grown in high-serum, high-glucose media, and both the $STHdh^{Q7}$ and $STHdh^{Q111}$ cells are very sensitive to seeding density; seeding the cells at too high or too low a density resulted in irreversible changes in proliferation as well as sensitivity to 3-NP. Finally, these cells are immortalized, which means that they have cancer cell properties as well as neuronal properties; this could confound findings related to cell signaling pathways that differ between neurons and cancer cells. It may be beneficial to perform experiments on primary cell cultures taken directly from the transgenic mouse model, or on the immortalized cell lines, but at the non-permissive temperature (39°C) for the temperature-sensitive SV40 large T antigen, to allow the cells to differentiate and behave more like neurons than cancer cells. This would ensure a uniform seeding density across experiments, and hopefully minimize the changes in protein expression levels.

4.7 Conclusions

This investigation provides further evidence of the neuroprotective properties of DMP in striatal cell lines, which are the most sensitive cell type to mHTT expression in HD patients. Additionally, this work shows, for the first time, that DMP is able to prevent the formation of Keap1- and Nrf2-positive inclusion bodies, which are correlated with cell death. At this time, the mechanism by which DMP exerts its protective effects remains unclear, although it seems likely that it involves the autophagosomal pathway or alterations in Keap1-Nrf2 protein interactions. Further study of direct protein interactions is warranted before definite claims are made. The findings presented here reveal a novel relationship between mHTT, Keap1, and Nrf2 and suggest that agents that modify the Nrf2-Keap1 signaling axis may have clinical relevance for treating HD.

References

Aiken, C. T., Tobin, A. J., & Schweitzer, E. S. (2004). A cell-based screen for drugs to treat Huntington's disease. *Neurobiology of disease*, *16*(3), 546-555.

Aiken, C. T., Tobin, A. J., & Schweitzer, E. S. (2004). A cell-based screen for drugs to treat Huntington's disease. *Neurobiology of disease*, *16*(3), 546-555.

Ambrose, C. M., Duyao, M. P., Barnes, G., Bates, G. P., Lin, C. S., Srinidhi, J., ... & MacDonald, M. E. (1994). Structure and expression of the Huntington's disease gene: evidence against simple inactivation due to an expanded CAG repeat. *Somatic cell and molecular genetics*, *20*(1), 27-38.

Ames, B. N., Shigenaga, M. K., & Hagen, T. M. (1993). Oxidants, antioxidants, and the degenerative diseases of aging. *Proceedings of the National Academy of Sciences*, *90*(17), 7915-7922.

Andrade, M. A., & Bork, P. (1995). HEAT repeats in the Huntington's disease protein. *Nature genetics*, *11*(2), 115-116.

Armstrong, M. J., & Miyasaki, J. M. (2012). Evidence-based guideline: Pharmacologic treatment of chorea in Huntington disease Report of the Guideline Development Subcommittee of the American Academy of Neurology.*Neurology*, *79*(6), 597-603.

Andrew, S. E., Goldberg, Y. P., Kremer, B., Telenius, H., Theilmann, J., Adam, S., ... & Hayden, M. R. (1993). The relationship between trinucleotide (CAG) repeat length and clinical features of Huntington's disease. *Nature genetics*,*4*(4), 398-403.

Auerbach, W., Hurlbert, M. S., Hilditch-Maguire, P., Wadghiri, Y. Z., Wheeler, V. C., Cohen, S. I., ... & Turnbull, D. H. (2001). The HD mutation causes progressive lethal neurological disease in mice expressing reduced levels of huntingtin. *Human Molecular Genetics*, *10*(22), 2515-2523.

Baliko, L., Csala, B., & Czopf, J. (2004). Suicide in Hungarian Huntington’s disease patients. *Neuroepidemiology*, *23*(5), 258-260.

Bartsch, H. (1997). DNA Adducts in Human Carcinogenesis. In *Selected Topics in Mass Spectrometry in the Biomolecular Sciences* (pp. 465-476). Springer Netherlands.

Bauer, P. O., Goswami, A., Wong, H. K., Okuno, M., Kurosawa, M., Yamada, M., ... & Nukina, N. (2010). Harnessing chaperone-mediated autophagy for the selective degradation of mutant huntingtin protein. *Nature biotechnology*, *28*(3), 256-263.

Beal, M. F., Brouillet, E., Jenkins, B. G., Ferrante, R. J., Kowall, N. W., Miller, J. M., ... & Hyman, B. T. (1993). Neurochemical and histologic characterization of striatal

excitotoxic lesions produced by the mitochondrial toxin 3-nitropropionic acid. *The Journal of Neuroscience*, *13*(10), 4181-4192.

Berlett, B. S., & Stadtman, E. R. (1997). Protein oxidation in aging, disease, and oxidative stress. *Journal of Biological Chemistry*, *272*(33), 20313-20316.

Browne, S. E., & Beal, M. F. (2006). Oxidative damage in Huntington's disease pathogenesis. *Antioxidants & redox signaling*, *8*(11-12), 2061-2073.

Bhide, P. G., Day, M., Sapp, E., Schwarz, C., Sheth, A., Kim, J., ... & DiFiglia, M. (1996). Expression of normal and mutant huntingtin in the developing brain. *The Journal of neuroscience*, *16*(17), 5523-5535.

Bonelli, R. M., & Hofmann, P. (2007). A systematic review of the treatment studies in Huntington's disease since 1990. *Expert Opinion Pharmacotherapy, 8*(2), 141-153.

Borlongan, C. V., Koutouzis, T. K., & Sanberg, P. R. (1997). 3-Nitropropionic acid animal model and Huntington's disease. *Neuroscience & Biobehavioral Reviews*, *21*(3), 289-293.

Brouillet, E., Hantraye, P., Ferrante, R. J., Dolan, R., Leroy-Willig, A., Kowall, N. W., & Beal, M. F. (1995). Chronic mitochondrial energy impairment produces selective striatal degeneration and abnormal choreiform movements in primates. *Proceedings of the National Academy of Sciences*, *92*(15), 7105-7109.

Bucciantini, M., Giannoni, E., Chiti, F., Baroni, F., Formigli, L., Zurdo, J., ... & Stefani, M. (2002). Inherent toxicity of aggregates implies a common mechanism for protein misfolding diseases. *Nature*, *416*(6880), 507-511.

Butterfield, D. A., & Kanski, J. (2001). Brain protein oxidation in age-related neurodegenerative disorders that are associated with aggregated proteins. *Mechanisms of ageing and development*, *122*(9), 945-962.

Calkins, M. J., Jakel, R. J., Johnson, D. A., Chan, K., Kan, Y. W., & Johnson, J. A. (2005). Protection from mitochondrial complex II inhibition in vitro and in vivo by Nrf2-mediated transcription. *Proceedings of the National Academy of Sciences of the United States of America*, *102*(1), 244-249.

Campbell, A. M. G., Corner, B., Norman, R. M., & Urich, H. (1961). The rigid form of Huntington's disease. *Journal of neurology, neurosurgery, and psychiatry*, *24*(1), 71.

Chang, D. T., Rintoul, G. L., Pandipati, S., & Reynolds, I. J. (2006). Mutant huntingtin aggregates impair mitochondrial movement and trafficking in cortical neurons. *Neurobiology of disease*, *22*(2), 388-400.

Chen, M., Ona, V. O., Li, M., Ferrante, R. J., Fink, K. B., Zhu, S., ... & Friedlander, R. M. (2000). Minocycline inhibits caspase-1 and caspase-3 expression and delays mortality in a transgenic mouse model of Huntington disease. *Nature medicine*, *6*(7), 797-801.

Claes, S., Van Zand, K., Legius, E., Dom, R., Malfroid, M., Baro, F., ... & Cassiman, J. J. (1995). Correlations between triplet repeat expansion and clinical features in Huntington's disease. *Archives of neurology*, *52*(8), 749-753.

Copple, I. M., Lister, A., Obeng, A. D., Kitteringham, N. R., Jenkins, R. E., Layfield, R., ... & Park, B. K. (2010). Physical and functional interaction of sequestosome 1 with Keap1 regulates the Keap1-Nrf2 cell defense pathway.*Journal of Biological Chemistry*, *285*(22), 16782-16788.

Cornett, J., Cao, F., Wang, C. E., Ross, C. A., Bates, G. P., Li, S. H., & Li, X. J. (2005). Polyglutamine expansion of huntingtin impairs its nuclear export. *Nature genetics*, *37*(2), 198-204.

Cumming, R. C., Andon, N. L., Haynes, P. A., Park, M., Fischer, W. H., & Schubert, D. (2004). Protein disulfide bond formation in the cytoplasm during oxidative stress. *Journal of Biological Chemistry*, *279*(21), 21749-21758.

Dasuri, K., Ebenezer, P., Zhang, L., Fernandez-Kim, S. O., Bruce-Keller, A. J., Markesbery, W. R., & Keller, J. N. (2010). Increased protein hydrophobicity in response to aging and Alzheimer disease. *Free Radical Biology and Medicine*,*48*(10), 1330-1337.

Dasuri, K., Zhang, L., & Keller, J. N. (2013). Oxidative stress, neurodegeneration, and the balance of protein degradation and protein synthesis. *Free Radical Biology and Medicine*, *62*, 170-185.

del Toro, D., Canals, J. M., Ginés, S., Kojima, M., Egea, G., & Alberch, J. (2006). Mutant huntingtin impairs the post-Golgi trafficking of brain-derived neurotrophic factor but not its Val66Met polymorphism. *The Journal of neuroscience*, *26*(49), 12748-12757.

Denny-Brown, D., & Porter, H. (1951). The effect of BAL (2, 3-dimercaptopropanol) on hepatolenticular degeneration (Wilson's disease). *New England Journal of Medicine*, *245*(24), 917-925.

Di Maio, L., Squitieri, F., Napolitano, G., Campanella, G., Trofatter, J. A., & Conneally, P. M. (1993). Onset symptoms in 510 patients with Huntington's disease. *Journal of medical genetics*, *30*(4), 289-292.

Di Maio, L., Squitieri, F., Napolitano, G., Campanella, G., Trofatter, J. A., & Conneally, P. M. (1993). Suicide risk in Huntington's disease. *Journal of medical genetics*, *30*(4), 293-295.

Dong, X., Zong, S., Witting, A., Lindenberg, K. S., Kochanek, S., & Huang, B. (2012). Adenovirus vector-based in vitro neuronal cell model for Huntington's disease with human disease-like differential aggregation and degeneration. *The journal of gene medicine*, *14*(7), 468-481.

Duff, K., Paulsen, J. S., Beglinger, L. J., Langbehn, D. R., Stout, J. C., & Predict-HD Investigators of the Huntington Study Group. (2007). Psychiatric symptoms in Huntington's disease before diagnosis: the predict-HD study. *Biological psychiatry*, *62*(12), 1341-1346.

Erdemoglu, A. K., & Boratav, C. (2002). Risperidone in chorea and psychosis of Huntington's disease. *European Journal of Neurology*, *9*(2), 182-183.

Ford, M. F. (1986). Treatment of depression in Huntington's disease with monoamine oxidase inhibitors. *The British Journal of Psychiatry*, *149*(5), 654-656.

Gauthier, L. R., Charrin, B. C., Borrell-Pagès, M., Dompierre, J. P., Rangone, H., Cordelières, F. P., ... & Saudou, F. (2004). Huntingtin controls neurotrophic support and survival of neurons by enhancing BDNF vesicular transport along microtubules. *Cell*, *118*(1), 127-138.

Graham, R. K., Deng, Y., Slow, E. J., Haigh, B., Bissada, N., Lu, G., ... & Hayden, M. R. (2006). Cleavage at the caspase-6 site is required for neuronal dysfunction and degeneration due to mutant huntingtin. *Cell*, *125*(6), 1179-1191.

Guidot, D. M., McCord, J. M., Wright, R. M., & Repine, J. E. (1993). Absence of electron transport (Rho 0 state) restores growth of a manganese-superoxide dismutase-deficient Saccharomyces cerevisiae in hyperoxia. Evidence for electron transport as a major source of superoxide generation in vivo. *Journal of Biological Chemistry*, *268*(35), 26699-26703.

Gusella, J. F., Wexler, N. S., Conneally, P. M., Naylor, S. L., Anderson, M. A., Tanzi, R. E., ... & Martin, J. B. (1983). A polymorphic DNA marker genetically linked to Huntingtons disease. *Nature*, *306*(5940), 234-238.

Hackam, A. S., Singaraja, R., Wellington, C. L., Metzler, M., McCutcheon, K., Zhang, T., ... & Hayden, M. R. (1998). The influence of huntingtin protein size on nuclear localization and cellular toxicity. *The Journal of cell biology*, *141*(5), 1097-1105.

He, X., & Ma, Q. (2010). Critical cysteine residues of Kelch-like ECH-associated protein 1 in arsenic sensing and suppression of nuclear factor erythroid 2-related factor 2. *Journal of Pharmacology and Experimental Therapeutics*,*332*(1), 66-75.

Heemskerk, A. W., & Roos, R. A. C. (2010). E04 Causes of death in Huntington's disease. *Journal of Neurology, Neurosurgery & Psychiatry*,*81*(Suppl 1), A22-A22.

Huntington, G. (1872). On Chorea. *Medical and Surgical Reporter of Philadelphia. 26*(15), 317-321.

Huntington Study Group. (2001). A randomized, placebo-controlled trial of coenzyme Q10 and remacemide in Huntington's disease. *Neurology*, *57*(3), 397-404.

Itoh, K., Wakabayashi, N., Katoh, Y., Ishii, T., O'Connor, T., & Yamamoto, M. (2003). Keap1 regulates both cytoplasmic-nuclear shuttling and degradation of Nrf2 in response to electrophiles. *Genes to Cells*, *8*(4), 379-391.

Jain, A. K., Bloom, D. A., & Jaiswal, A. K. (2005). Nuclear import and export signals in control of Nrf2. *Journal of Biological Chemistry*, *280*(32), 29158-29168.

Jang, M., & Cho, I. H. (2015). Sulforaphane Ameliorates 3-Nitropropionic Acid-Induced Striatal Toxicity by Activating the Keap1-Nrf2-ARE Pathway and Inhibiting the MAPKs and NF-κB Pathways. Molecular neurobiology, 1-17.

Karapetian, R. N., Evstafieva, A. G., Abaeva, I. S., Chichkova, N. V., Filonov, G. S., Rubtsov, Y. P., ... & Vartapetian, A. B. (2005). Nuclear oncoprotein prothymosin α is a partner of Keap1: implications for expression of oxidative stress-protecting genes. *Molecular and cellular biology*, *25*(3), 1089-1099.

Kensler, T. W., Wakabayashi, N., & Biswal, S. (2007). Cell survival responses to environmental stresses via the Keap1-Nrf2-ARE pathway. *Annu. Rev. Pharmacol. Toxicol.*, *47*, 89-116.

Kirkwood, S. C., Su, J. L., Conneally, P. M., & Foroud, T. (2001). Progression of symptoms in the early and middle stages of Huntington disease. *Archives of Neurology*, *58*(2), 273-278.

Komatsu, M., Kurokawa, H., Waguri, S., Taguchi, K., Kobayashi, A., Ichimura, Y., ... & Yamamoto, M. (2010). The selective autophagy substrate p62 activates the stress responsive transcription factor Nrf2 through inactivation of Keap1. *Nature cell biology*, *12*(3), 213-223.

Kobayashi, A., Kang, M. I., Okawa, H., Ohtsuji, M., Zenke, Y., Chiba, T., ... & Yamamoto, M. (2004). Oxidative stress sensor Keap1 functions as an adaptor for Cul3-based E3 ligase to regulate proteasomal degradation of Nrf2. *Molecular and cellular biology*, *24*(16), 7130-7139.

Landles, C., & Bates, G. P. (2004). Huntingtin and the molecular pathogenesis of Huntington's disease. *EMBO reports*, *5*(10), 958-963.

Lau, A., Tian, W., Whitman, S. A., & Zhang, D. D. (2013). The predicted molecular weight of Nrf2: it is what it is not. *Antioxidants & redox signaling*, *18*(1), 91-93.

Lau, A., Wang, X. J., Zhao, F., Villeneuve, N. F., Wu, T., Jiang, T., ... & Zhang, D. D. (2010). A noncanonical mechanism of Nrf2 activation by autophagy deficiency: direct interaction between Keap1 and p62. *Molecular and cellular biology*, *30*(13), 3275-3285.

Lau, A., Whitman, S. A., Jaramillo, M. C., & Zhang, D. D. (2013). Arsenic‐Mediated Activation of the Nrf2‐Keap1 Antioxidant Pathway. *Journal of biochemical and molecular toxicology*, *27*(2), 99-105.

Leavitt, B. R., Guttman, J. A., Hodgson, J. G., Kimel, G. H., Singaraja, R., Vogl, A. W., & Hayden, M. R. (2001). Wild-type huntingtin reduces the cellular toxicity of mutant huntingtin in vivo. *The American Journal of Human Genetics*, *68*(2), 313-324.

Leavitt, B. R., Raamsdonk, J. M., Shehadeh, J., Fernandes, H., Murphy, Z., Graham, R. K., ... & Hayden, M. R. (2006). Wild‐type huntingtin protects neurons from excitotoxicity. *Journal of neurochemistry*, *96*(4), 1121-1129.

Li, S. H., & Li, X. J. (2004). Huntingtin–protein interactions and the pathogenesis of Huntington's disease. *TRENDS in Genetics*, *20*(3), 146-154.

Lin, M. T., & Beal, M. F. (2006). Mitochondrial dysfunction and oxidative stress in neurodegenerative diseases. *Nature*, *443*(7113), 787-795.

Lipe, H., & Bird, T. (2009). Late onset Huntington Disease: clinical and genetic characteristics of 34 cases. *Journal of the neurological sciences*, *276*(1), 159-162.

MacDonald, M. E., Ambrose, C. M., Duyao, M. P., Myers, R. H., Lin, C., Srinidhi, L., ... & Swaroop, M. (1993). A novel gene containing a trinucleotide repeat that is expanded and unstable on Huntington's disease chromosomes. *Cell*, *72*(6), 971-983.

Mariani, E., Polidori, M. C., Cherubini, A., & Mecocci, P. (2005). Oxidative stress in brain aging, neurodegenerative and vascular diseases: an overview.*Journal of Chromatography B*, *827*(1), 65-75.

Martínez, A., Portero‐Otin, M., Pamplona, R., & Ferrer, I. (2010). Protein targets of oxidative damage in human neurodegenerative diseases with abnormal protein aggregates. *Brain Pathology*, *20*(2), 281-297.

Montine, T. J., Beal, M. F., Robertson, D., Cudkowicz, M. E., Biaggioni, I., O'Donnell, H., ... & Morrow, J. D. (1999). Cerebrospinal fluid F2-isoprostanes are elevated in Huntington's disease. *Neurology*, *52*(5), 1104-1104.

Moosmann, B., & Behl, C. (2002). Antioxidants as treatment for neurodegenerative disorders. *Expert opinion on investigational drugs*, *11*(10), 1407-1435.

Nance, M. A., & Myers, R. H. (2001). Juvenile onset Huntington's disease—clinical and research perspectives. *Mental retardation and developmental disabilities research reviews*, *7*(3), 153-157.

Nasir, J., Floresco, S. B., O'Kusky, J. R., Diewert, V. M., Richman, J. M., Zeisler, J., ... & Hayden, M. R. (1995). Targeted disruption of the Huntington's disease gene results in

embryonic lethality and behavioral and morphological changes in heterozygotes. *Cell*, *81* (5), 811-823.

Neilsen, J. M., & Butt, E. M. (1955). Treatment of Huntington's chorea with bal. *Bull. Los Angel Neuro Soc.* 20, 38-39.

Neuwald, A. F., & Hirano, T. (2000). HEAT repeats associated with condensins, cohesins, and other complexes involved in chromosome-related functions. *Genome research*, *10*(10), 1445-1452.

Nguyen, T., Yang, C. S., & Pickett, C. B. (2004). The pathways and molecular mechanisms regulating Nrf2 activation in response to chemical stress. *Free Radical Biology and Medicine*, *37*(4), 433-441.

Nguyen, T., Sherratt, P. J., Nioi, P., Yang, C. S., & Pickett, C. B. (2005). Nrf2 controls constitutive and inducible expression of ARE-driven genes through a dynamic pathway involving nucleocytoplasmic shuttling by Keap1. *Journal of Biological Chemistry*, *280*(37), 32485-32492.

Ossato, G., Digman, M. A., Aiken, C., Lukacsovich, T., Marsh, J. L., & Gratton, E. (2010). A two-step path to inclusion formation of huntingtin peptides revealed by number and brightness analysis. *Biophysical journal*, *98*(12), 3078-3085.

Pankiv, S., Clausen, T. H., Lamark, T., Brech, A., Bruun, J. A., Outzen, H., ... & Johansen, T. (2007). p62/SQSTM1 binds directly to Atg8/LC3 to facilitate degradation of ubiquitinated protein aggregates by autophagy. *Journal of Biological Chemistry*, *282*(33), 24131-24145

Panov, A. V., Gutekunst, C. A., Leavitt, B. R., Hayden, M. R., Burke, J. R., Strittmatter, W. J., & Greenamyre, J. T. (2002). Early mitochondrial calcium defects in Huntington's disease are a direct effect of polyglutamines. *Nature neuroscience*, *5*(8), 731-736.

Paupe, V., Dassa, E. P., Goncalves, S., Auchère, F., Lonn, M., Holmgren, A., & Rustin, P. (2009). Impaired nuclear Nrf2 translocation undermines the oxidative stress response in Friedreich ataxia. *PLoS One*, *4*(1), e4253.

Pérez-Severiano, F., Ríos, C., & Segovia, J. (2000). Striatal oxidative damage parallels the expression of a neurological phenotype in mice transgenic for the mutation of Huntington's disease. *Brain research*, *862*(1), 234-237.

Pérez-Severiano, F., Santamaría, A., Pedraza-Chaverri, J., Medina-Campos, O. N., Ríos, C., & Segovia, J. (2004). Increased formation of reactive oxygen species, but no changes in glutathione peroxidase activity, in striata of mice transgenic for the Huntington's disease mutation. *Neurochemical research*,*29*(4), 729-733.

Perutz, M. F., Johnson, T., Suzuki, M., & Finch, J. T. (1994). Glutamine repeats as polar zippers: their possible role in inherited neurodegenerative diseases.*Proceedings of the National Academy of Sciences*, *91*(12), 5355-5358.

Pitts, A., Dailey, K., Newington, J. T., Chien, A., Arseneault, R., Cann, T., ... & Cumming, R. C. (2012). Dithiol-based compounds maintain expression of antioxidant protein peroxiredoxin 1 that counteracts toxicity of mutant huntingtin.*Journal of Biological Chemistry*, *287*(27), 22717-22729.

Porter, N. A. (1986). Mechanisms for the autoxidation of polyunsaturated lipids. *Accounts of Chemical Research*, *19*(9), 262-268.

Ramsey, C. P., Glass, C. A., Montgomery, M. B., Lindl, K. A., Ritson, G. P., Chia, L. A., ... & Jordan-Sciutto, K. L. (2007). Expression of Nrf2 in neurodegenerative diseases. *Journal of neuropathology and experimental neurology*, *66*(1), 75.

Ranen, N. G., Peyser, C. E., Coyle, J. T., Bylsma, F. W., Sherr, M., Day, L., ... & Folstein, S. E. (1996). A controlled trial of idebenone in Huntington's disease. *Movement disorders*, *11*(5), 549-554.

Ribaï, P., Nguyen, K., Hahn-Barma, V., Gourfinkel-An, I., Vidailhet, M., Legout, A., ... & Dürr, A. (2007). Psychiatric and cognitive difficulties as indicators of juvenile huntington disease onset in 29 patients. *Archives of neurology*, *64*(6), 813-819.

Ruocco, H. H., Lopes-Cendes, I., Li, L. M., Santos-Silva, M., & Cendes, F. (2006). Striatal and extrastriatal atrophy in Huntington's disease and its relationship with length of the CAG repeat. *Brazilian journal of medical and biological research*, *39*(8), 1129-1136.

Ryu, H., Rosas, H. D., Hersch, S. M., & Ferrante, R. J. (2005). The therapeutic role of creatine in Huntington's disease. *Pharmacology & therapeutics*, *108*(2), 193-207.

Sanberg, P. R., Fibiger, H. C., & Mark, R. F. (1981). Body weight and dietary factors in Huntington's disease patients compared with matched controls. *The Medical Journal of Australia*, *1*(8), 407-409.

Schreibelt, G., Van Horssen, J., Van Rossum, S., Dijkstra, C. D., Drukarch, B., & de Vries, H. E. (2007). Therapeutic potential and biological role of endogenous antioxidant enzymes in multiple sclerosis pathology. *Brain research reviews*, *56*(2), 322-330.

Sena, L. A., & Chandel, N. S. (2012). Physiological roles of mitochondrial reactive oxygen species. *Molecular cell*, *48*(2), 158-167.

Shih, A. Y., Imbeault, S., Barakauskas, V., Erb, H., Jiang, L., Li, P., & Murphy, T. H. (2005). Induction of the Nrf2-driven antioxidant response confers neuroprotection during mitochondrial stress in vivo. *Journal of Biological Chemistry*, *280*(24), 22925-22936.

Shringarpure, R., Grune, T., & Davies, K. J. A. (2001). Protein oxidation and 20S proteasome-dependent proteolysis in mammalian cells. *Cellular and Molecular Life Sciences*, *58*(10), 1442-1450.

Slow, E. J., Graham, R. K., & Hayden, M. R. (2006). To be or not to be toxic: aggregations in Huntington and Alzheimer disease. *Trends in Genetics*, *22*(8), 408-411.

Strong, T. V., Tagle, D. A., Valdes, J. M., Elmer, L. W., Boehm, K., Swaroop, M., ... & Albin, R. L. (1993). Widespread expression of the human and rat Huntington's disease gene in brain and nonneural tissues. *Nature genetics*, *5*(3), 259-265.

Suzanne, M., Vonsattel, J. P., & Richardson Jr, E. P. (1988). Morphometric demonstration of atrophic changes in the cerebral cortex, white matter, and neostriatum in Huntington's disease. *Journal of Neuropathology & Experimental Neurology*, *47*(5), 516-525.

Takano, H., & Gusella, J. F. (2002). The predominantly HEAT-like motif structure of huntingtin and its association and coincident nuclear entry with dorsal, an NF-kB/Rel/dorsal family transcription factor. *BMC neuroscience*, *3*(1), 15.

Tanji, K., Maruyama, A., Odagiri, S., Mori, F., Itoh, K., Kakita, A., ... & Wakabayashi, K. (2013). Keap1 is localized in neuronal and glial cytoplasmic inclusions in various neurodegenerative diseases. *Journal of Neuropathology & Experimental Neurology*, *72*(1), 18-28.

Trejo, A., Tarrats, R. M., Alonso, M. E., Boll, M. C., Ochoa, A., & Velásquez, L. (2004). Assessment of the nutrition status of patients with Huntington's disease. *Nutrition*, *20*(2), 192-196.

Trettel, F., Rigamonti, D., Hilditch-Maguire, P., Wheeler, V. C., Sharp, A. H., Persichetti, F., ... & MacDonald, M. E. (2000). Dominant phenotypes produced by the HD mutation in STHdhQ111 striatal cells. *Human molecular genetics*, *9*(19), 2799-2809.

Trushina, E., Dyer, R. B., Badger, J. D., Ure, D., Eide, L., Tran, D. D., ... & McMurray, C. T. (2004). Mutant huntingtin impairs axonal trafficking in mammalian neurons in vivo and in vitro. *Molecular and cellular biology*, *24*(18), 8195-8209.

Valko, M., Izakovic, M., Mazur, M., Rhodes, C. J., & Telser, J. (2004). Role of oxygen radicals in DNA damage and cancer incidence. *Molecular and cellular biochemistry*, *266*(1-2), 37-56.

Van Raamsdonk, J. M., Murphy, Z., Slow, E. J., Leavitt, B. R., & Hayden, M. R. (2005). Selective degeneration and nuclear localization of mutant huntingtin in the YAC128 mouse model of Huntington disease. *Human molecular genetics*,*14*(24), 3823-3835.

Villeneuve, N. F., Lau, A., & Zhang, D. D. (2010). Regulation of the Nrf2–Keap1 antioxidant response by the ubiquitin proteasome system: an insight into cullin-ring ubiquitin ligases. *Antioxidants & redox signaling*, *13*(11), 1699-1712.

Vonsattel JP, DiFiglia M (1998) Huntington disease. J Neuropathol Exp Neurol 57(5):369–384

Wexler, N. S., Young, A. B., Tanzi, R. E., Travers, H., Starosta-Rubinstein, S., Penney, J. B., ... & Gusella, J. F. (1987). Homozygotes for Huntington's disease. *Nature*, *326*(6109), 194-197.

White, J. K., Auerbach, W., Duyao, M. P., Vonsattel, J. P., Gusella, J. F., Joyner, A. L., & MacDonald, M. E. (1997). Huntingtin is required for neurogenesis and is not impaired by the Huntington's disease CAG expansion.*Nature genetics*, *17*(4), 404-410.

Xia, J., Lee, D. H., Taylor, J., Vandelft, M., & Truant, R. (2003). Huntingtin contains a highly conserved nuclear export signal. *Human molecular genetics*,*12*(12), 1393-1403.

Yu, M., Li, H., Liu, Q., Liu, F., Tang, L., Li, C., ... & Yang, X. (2011). Nuclear factor p65 interacts with Keap1 to repress the Nrf2-ARE pathway. *Cellular signalling*, *23*(5), 883-892.

Zainelli, G. M., Dudek, N. L., Ross, C. A., Kim, S. Y., & Muma, N. A. (2005). Mutant huntingtin protein: a substrate for transglutaminase 1, 2, and 3. *Journal of Neuropathology & Experimental Neurology*, *64*(1), 58-65.

Zala, D., Colin, E., Rangone, H., Liot, G., Humbert, S., & Saudou, F. (2008). Phosphorylation of mutant huntingtin at S421 restores anterograde and retrograde transport in neurons. *Human molecular genetics*, *17*(24), 3837-3846.

Zeitlin, S., Liu, J. P., Chapman, D. L., Papaioannou, V. E., & Efstratiadis, A. (1995). Increased apoptosis and early embryonic lethality in mice nullizygous for the Huntington's disease gene homologue. *Nature genetics*, *11*(2), 155-163.

Zhang, Y., Li, M., Drozda, M., Chen, M., Ren, S., Mejia Sanchez, R. O., ... & Friedlander, R. M. (2003). Depletion of wild‐type huntingtin in mouse models of neurologic diseases. *Journal of neurochemistry*, *87*(1), 101-106.

Zhao, J., Kobori, N., Aronowski, J., & Dash, P. K. (2006). Sulforaphane reduces infarct volume following focal cerebral ischemia in rodents. *Neuroscience letters*, *393*(2), 108-112.

Zuccato, C., Ciammola, A., Rigamonti, D., Leavitt, B. R., Goffredo, D., Conti, L., ... & Cattaneo, E. (2001). Loss of huntingtin-mediated BDNF gene transcription in Huntington's disease. *Science*, *293*(5529), 493-498.

Appendix

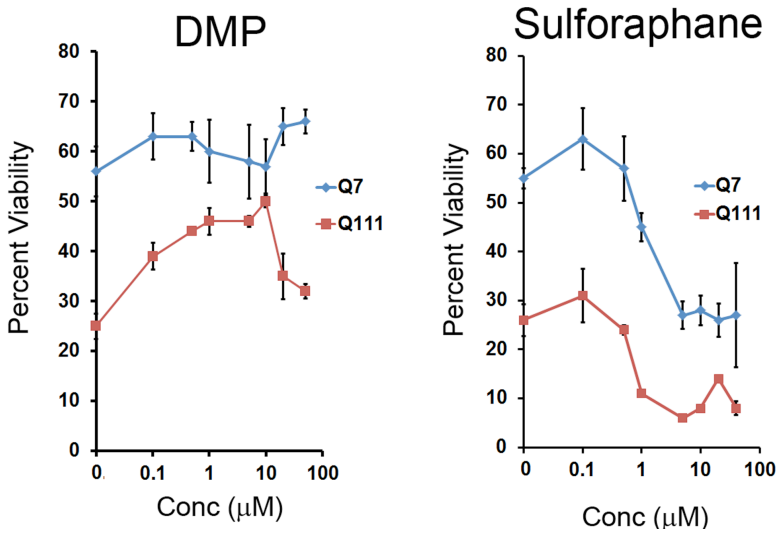

Appendix: Figure I. Canonical activator Sulforaphane did not protect against mHTT toxicity. The abilities of 2,3-dimercaptopropanol (DMP) and sulforaphane (SFN) to protect against 3-NP-induced toxicity in the striatal cell lines were assessed by MTT assay. Following a 24-hour treatment with 10mM 3-NP, DMP enhanced viability in the STHdh^{Q111} cells with an optimal concentration of 10μM. Sulforaphane (a classical Nrf2 activator) was not protective and potentiated 3-NP-induced toxicity at concentrations above 0.5μM. Error bars represent the standard error of the mean cell viability obtained from four replicates derived one independent experiment.

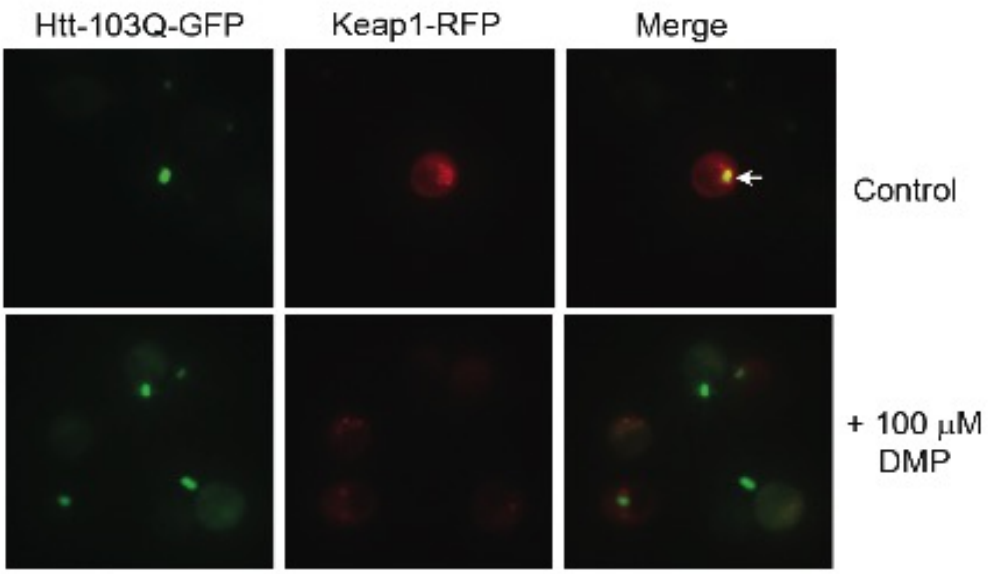

Appendix: Figure II. mHTT and Keap1 co-localize in puncta. Fluorescence microscopy of live PC12 cells co-expressing mHTT fused to GFP (Htt-103Q-GFP) and Keap1 fused to RFP (Keap1-RFP) revealed co-localization of both proteins in large perinuclear structures that resemble aggresomes. Treatment with DMP (bottom panels) led to a sharp decrease in co-localization of Keap1 with mHTT and the appearance of smaller Keap1 puncta.

Bull Los Angel Neuro Soc 1955 20(1) 38-39

TREATMENT OF HUNTINGTON'S CHOREA WITH BAL*

J. M. Nielsen, M.D. and E. M. Butt, M.D.

When it became apparent that BAL was of some benefit in hepatolenticular degeneration and it seemed that the benefit was due to elimination of copper from the body, it occurred to the writers that other diseases of the basal ganglia might possibly be due to a disorder of metal metabolism. Several cases of paralysis agitans have been started on dimercaptopropanol; but because of the discomfort and the difficulties of administration, the work in each instance has come to a standstill. Several cases of Huntington's chorea have also been treated but in only two cases has it been consistent. It is acknowledged that the dose is inadequate, but the pragmatic limitations determine how much can be given.

REPORT OF CASES

Case 1. *Woman of 29 years with Huntington's chorea. Treated with BAL. Distinct improvement in 14 months.*

Mrs. J. E., aged 29 years, mother of two children, 3 and 1 year respectively, was brought for examination by her husband on May 29, 1953, because of general fatigue and irritability, large appetite without gain in weight and clumsiness, all of about three years' duration. She had had a tonsillectomy and appendectomy, measles, mumps, pertussis and a light case of influenza. Following one of her illnesses, she was said to have a murmur of the heart and was confined to her home for six months.

Her own history was to the effect that her first symptoms had appeared after the birth of her first child three years before. She stated that she had always had an enormous appetite and now craved sweets. She would get up at night and eat anything sweet, such as raisins, which she might have on hand for cooking. She added that members of her own family were all big eaters. In spite of this bulimia she did not gain weight. She was tired and irritable all the time but had been examined for diabetes with negative results.

She also complained of numbness and "going to sleep" of the left hand, including all of the fingers. Her clumsiness was recognized by her, but she stated she had always been clumsy. She complained of muscular cramps at night, especially in the thighs. She had quit smoking when her child was born but she then began to eat candy, mostly at night and as much as three pounds a night. She added that before the time of the birth of her first baby she had attacks of profuse perspiration with flushing, rapid pulse and high blood pressure. This cleared with a pregnancy and miscarriage.

Physical examination disclosed a well-nourished but not obese woman of 29 years with a temperature of 98.3° F. The thyroid gland was not palpable. The heart was normal and without murmur. Blood pressure was 130 systolic and 70 diastolic, and the pulse rate 90 per minute. The brachial arteries were palpable but not sclerosed.

Neurological examination showed a silly-acting woman with generalized choreo-athetoid movements and facial grimacing like Huntington's chorea. The sense of smell, visual fields and fundi were normal. The pupils were 4 mm. each, regular, and active in response to light and convergence. Her hearing was excellent. As the patient noted the movements, she said, "I have extracurricular movements." She grinned and grimaced as she said it with a giggle. The grip was unsustained and she dropped small articles she tried to hold. The deep reflexes were all small and hardly obtainable, except the right knee jerk and the Achilles reflexes which were normal. Sensory perception was unimpaired.

On the suspicion that Huntington's chorea might be a disturbance of heavy metal metabolism, it was decided to hospitalize her and give her as much BAL ($2\frac{1}{2}$ mg. per kg.) as her buttocks would tolerate. In two months she gained 30 pounds (13.6 kilos) in weight, lost her bulimia and looked a great deal better. She was returned to her home and continued one dose per day, alternating the two hips, two weeks on and two weeks off each time.

* From the Department of Medicine (Neurology), University of California at Los Angeles and the Department of Pathology, Los Angeles General Hospital, Los Angeles, California.

On re-examination Sept. 1, 1954, the movements were greatly diminished and her grip was normal for a woman, right 68 and left 59; but she still could not maintain a grip. She was euphoric and had peculiar head postures; but there was much less grimacing, no tongue involvement and few abnormal movements of the hands.

Blood copper and lead determinations were made before treatment was begun. On the whole blood, lead was .036 mg. per 100 Ml. while copper was 0.267. On the serum, the values were lead .013 and copper .196 mg. per Ml. For lack of information these values cannot be interpreted as yet. Some authors (1) consider a *low* copper value to be evidence of disease because of fixation of it in the nervous system. Others consider a high value (as in this case) abnormal. The writers are therefore simply recording this data.

Case 2. *Woman aged 52 years with involuntary writhing movements for seven years. Normal deep reflexes. No pathological toe signs. Elevated blood copper concentration. Clinical improvement in 10 months.*

Mrs. H. O., a white woman aged 52 years without family history, even in collaterals, of anything resembling Huntington's chorea, came Dec. 29, 1952, with complaint of generalized involuntary movements for about seven years. She had two brothers and one sister all living and well, but she had never had any children. Her own past history was brief, having had tonsillitis, measles, mumps, chicken pox, diphtheria, pneumonia and influenza, but no surgery or accidents. Menopause had been established at age 50.

At the age of about 45 years, she noted writhing movements of one foot. After a few months similar movements appeared in the other foot and then the hands became involved. She was still able to walk and even to sew, but she had difficulty in buttoning her clothes and holding a cup of coffee. She had no dysphagia but her speech was affected by imperfect control of the tongue. In walking she could not hold to a line and had fallen a number of times.

Physical examination showed a well-nourished woman with an essentially normal cardiovascular system, blood pressure of 162 systolic and 86 diastolic and a pulse rate of 78 per minute. The liver was not enlarged.

Neurological examination showed a normal sense of smell, normal visual fields and fundi. The pupils were 4 mm. and equal, active in response to light and convergent. The hearing was slightly diminished in both ears, but more on the left side. The Weber was referred to the right; the Rinne was normal. There was much grimacing and tongue movement, as well as athetoid movement and posture of the fingers and also writhing of the lower limbs. The grip could not be maintained. All deep reflexes were normal, but the plantar response was absent bilaterally. Sensory perception was unimpaired. Serum copper concentration was found to be 0.220 mg. per 100 Ml. of serum.

She was treated with as much BAL as her buttocks would tolerate. On July 14, 1953, the husband reported that the patient had improved to the extent of being able to drive the car a short distance but that she was paranoid and delusional. On Oct. 8, 1953, the patient was better mentally. She was taking one injection daily, 2½ mg. per kg. However, she had had a number of sterile abscesses of the buttocks, both of which were scarred. Still she was willing to continue because she recognized the improvement.

In view of these clinical results, the two cases are considered worthy of report in the hope that others will try the treatment.

SUMMARY

In two cases of Huntington's chorea, both with high blood copper concentration, there was definite clinical improvement on treatment with BAL for 12 and 14 months respectively. No conclusions can be drawn relative to the part played by copper in the syndrome. It is hoped to stimulate others to try the method, which has serious drawbacks because of the necessity for continued use of the buttocks for intramuscular injection, though the theoretical amounts of BAL required cannot be given.

REFERENCE

SULLIVAN, F. L., MARTIN, H. L. AND FLETCHER, M.: Wilson's disease (hepatolenticular degeneration). A family study. Arch. Neurol. & Psychiat. 69:756–759 (June) 1953.

Appendix: Figure III. Neilsen, J. M., & Butt, E. M. (1955). Treatment of Huntington's chorea with bal. *Bull. Los Angel Neuro Soc.* 20, 38-39.

Margaret Lauren Tindale

POST-SECONDARY EDUCATION

Master of Science, Neuroscience Candidate
Western University
London, ON, Canada
2013 – 2015

Bachelor of Science, Honors Double Major in Biology & Medical Cell Biology
Western University
London, ON, Canada
2007 – 2013

EMPLOYMENT

Teaching Assistant
Introductory Psychology (PSYCH 1000) & Integrated Neuroscience (ACB 4451A)
Western University
London, ON, Canada
2014 – 2015

LABORATORY EXPERIENCE

Graduate Student
Supervisor: Dr. Robert Cumming
Western University
London, ON, Canada
2013 – 2015

PUBLICATIONS

RA Harris, L Tindale, and RC Cumming. "Age-dependent metabolic dysregulation in cancer and Alzheimer's disease." *Biogerontology* (2014): 1-19.

POSTER PRESENTATIONS

L Tindale, K Dailey, RC Cumming. (November, 2014) Mutant Huntingtin mediated repression of antioxidant gene expression is rescued by a novel Nrf2 activating agent. *Society for Neuroscience's 44th Annual Meeting.* Washington, DC

L Tindale, K Dailey, RC Cumming. (May, 2014) Non-canonical activation of Nrf2 as a potential therapy for Huntington's Disease. *34th Annual Meeting of the Southern Ontario Neuroscience Association.* Western University, London, Ontario